Université Abou Moumouni

Doctoral Research Program on Climate Change and Energy (DRP-CCE)

NIGER

INTERNATIONAL MASTER'S PROGRAM IN RENEWABLE ENERGY AND GREEN HYDROGEN

SPECIALITY: PHOTOVOLTAICS FOR GREEN HYDROGEN TECHNOLOGY

MASTER'S THESIS TOPIC:

Test of Different Instruments for Measuring the Current/Voltage-Curve of Photovoltaic Modules

Presented on the 19th of August, 2023, by: **Preston Nyanamah**

Supervisors in Germany

1. **Prof. Dr. Jurgen H. Werner**

   Institute for Photovoltaics,
   University of Stuttgart, Germany

2. **Prof. Dr. Uwe Rau**

   IEK-5, Forschungszentrum
   Julich, Germany

Local Supervisor

1. **Assoc. Prof. Mounkaila Saley. Moussa**

   Université Abdou Moumouni of Niamey, Niger

Thesis defense Committee Members:

1. **President:** Prof. Madougou Saidou
   Université Abdou Moumouni of Niamey, Niger

2. **Examinator :** Dr. Souley Kallo Moutari
   Université Abdou Moumouni of Niamey, Niger

Academic year: 2022-2023

Dedication:

I dedicate this thesis to my late father, Augustine V. Nyanamah, who, despite his modest income, ensured that I acquired a solid childhood education from the best schools.

To my mother, Roseline Garteh, I love you dearly. You thought me how to read and write long before my teachers. I dedicate this thesis to you because I owe it to you.

To my uncle, Prince Nyanamah, you are my academic champion. I am forever grateful to you for teaching me academic excellence. I do not know anyone who hypes and celebrates me better than you. You have been my biggest supporter and number one motivator since my childhood. This thesis is dedicated to you.

Acknowledgment

Abstract

Nowadays, there is a high demand for energy worldwide. Solar energy has emerged as one of the best renewable energy options to help meet global energy demands while helping to solve the climate change crisis. The rising demand for solar energy has prompted the massive production and widespread deployment of solar PV modules globally. Manufacturers, researches, engineers and solar installers use specialized instruments known as solar PV current/voltage testers or tracers to test and measure the current/voltage characteristics of Solar modules. Such measurement enables fault detection and performance problems in solar modules; however, they are very expensive and often inaccessible for institutions and researchers with low income. In certain cases, low-cost instruments are developed as alternatives to test solar PV performance issues. Performance problems in solar modules are caused by changes in the modules' parameters such as series resistance, parallel resistance, ideality factor and saturation current density. Solar module parameters are very crucial but difficult to compute. Thus, the main goal of this study was to test both commercial and low-cost solar module current/voltage testers by measuring the current/voltage curves of solar modules and using the current/voltage data to calculate solar modules and cells parameters. The Werner plots were used along with the Origin software to evaluate solar module/cells parameters. The research results showed that the low-cost solar module current/voltage curve tester can compete with commercial current/voltage tester in terms of measuring series resistance, parallel resistance, saturation current density, etc. Furthermore, it was confirmed that the low-cost instrument can measure multiple solar modules at once, a capability that was lacking in the expensive commercial WaveLabs instrument. However, the commercial instruments were faster in measuring the modules current/voltage curve due to their short sweep speed (20-500μs) and (0.02-2s) respectively compared to a sweep speed of 6seconds for the low-cost instrument.

Key words: Solar PV Modules, Current/Voltage Curve Testers, Solar Module Parameters.

Résumé

De nos jours, la demande d'énergie est très forte dans le monde entier. L'énergie solaire s'est imposée comme l'une des meilleures options en matière d'énergie renouvelable pour répondre à la demande mondiale d'énergie tout en contribuant à résoudre la crise du changement climatique. La demande croissante d'énergie solaire a entraîné la production massive et le déploiement à grande échelle de modules solaires photovoltaïques dans le monde entier. Les fabricants, les chercheurs, les ingénieurs et les installateurs solaires utilisent des instruments spécialisés, appelés testeurs ou traceurs de courant/tension PV, pour tester et mesurer les caractéristiques de courant/tension des modules solaires. Ces mesures permettent de détecter les défauts et les problèmes de performance des modules solaires, mais elles sont très coûteuses et souvent inaccessibles aux institutions et aux chercheurs à faibles revenus. Dans certains cas, des instruments peu coûteux sont développés comme alternatives pour tester les problèmes de performance des modules solaires photovoltaïques. Les problèmes de performance des modules solaires sont causés par des changements dans les paramètres des modules tels que la résistance en série, la résistance en parallèle, le facteur d'idéalité et la densité du courant de saturation. Les paramètres des modules solaires sont très importants mais difficiles à calculer. L'objectif principal de cette étude est donc de tester des testeurs de courant/tension des modules solaires commerciaux et bons marchés en mesurant les courbes de courant/tension des modules solaires et en utilisant les données de courant/tension pour calculer les paramètres des modules et des cellules solaires. Les tracés de Werner ont été utilisés avec le logiciel Origin pour évaluer les paramètres des modules/cellules solaires. Les résultats de la recherche ont montré que le testeur des courbes de courant/tension des modules solaires bons marchés peut rivaliser avec les testeurs de courant/tension commerciaux en termes de mesure: de la résistance en série et, en parallèle, de la densité du courant de saturation, etc. En outre, il a été confirmé que l'instrument bon marché peut mesurer plusieurs modules solaires à la fois, une capacité qui faisait défaut à l'instrument commercial coûteux de WaveLabs. Cependant, les instruments commerciaux étaient plus rapides pour mesurer la courbe de courant/tension des modules en raison de leur vitesse de balayage courte (20-500μs) et (0,02-2s) respectivement, par rapport à une vitesse de balayage de 6 secondes pour l'instrument à faible coût.

Mots clés: Modules Solaires Photovoltaïques, Testeurs de Courbes de Courant/Tension, Paramètres des Modules Solaires.

Acronyms and abbreviations

WASCAL: West African Science Service Center on Climate Change and Adapted Land

BMBF: Bundesministerium Fur Bildung und Forschung

PV: Photovoltaic

ipv: Institute for Photovoltaic

DC: Direct Current

MOSFET: Metal oxide semiconductor field effect transistor

V_{OC}: Open circuit voltage

k_B : Boltzmann constant

J_{SC}: Short circuit current density

MPP: Maximum Power Point

I_{ph} : Photocurrent

R_S : Series Resistance

R_P : Parallel Resistance

J_0 : Saturation current density

J_{ph}: Short Circuit Density

J_d: Diode Current

n: ideality factor

G_{oc}: conductance at open circuit condition

R_{oc}: Resistance at open circuit condition

R_{ch}: Characteristic Resistance

List of tables

List of figures

TABLE OF CONTENTS

Chapter 1: Introduction

1.1 Background and significance of the study

By the year 2030, 80% of global electricity production will come from renewable energy (Kongphet *et al*., 2022), and Photovoltaics will become the key driver of this advancement (World Energy Outlook, 2020). Photovoltaics, widely known as solar PV, is the science and technology of the conversion of solar energy directly into electrical power. This phenomenon occurs when photons of light strike the surface of semiconducting devices such as solar cells or modules. Globally, Solar PV technology has gained tremendous interests and widespread applications because of its proven results in combating climate change, providing clean and affordable energy for mankind while helping to curb societal dependance on fossil fuels.

The solar PV industry has grown rapidly over the last couple of decades (Das, 2016) and comes third in order of importance and total power production capacity after hydroelectricity and wind power (Bai et al., 2014). Bellini (2020) has reported that the total installed capacity of grid-tied solar PV and Stand-Alone solar PV worldwide stood at 580.1 Giga-Watt peak (GWp) and 3.4 Giga-Watt peak (GWp) in 2019, respectively (BELLINI, 2020) while (Kongphet *et al*., 2022) reported a 760 GW worldwide PV installation in 2020, indicating a massive increment of more than 139GW compared to the year 2019.The rapid growth of the solar PV industry has given rise to the annual manufacture and deployment of millions of solar PV modules worldwide.

The simplest, most representative unit of a PV module is known as a solar cell. PV modules are produced by means of wiring multiple cells in series or parallel, resulting in an increase in the output voltage for series connections and an increase in the output current for parallel connections. One of the merits of photovoltaics technology is its durability. Manufacturers typically stipulate a warranty of about 25 years for modules using enhanced indoor lifecycle test (Leite *et al.*, 2013) which are usually carried out under standard testing conditions (STC). However, over this period, the performance of solar modules degrades gradually due to outdoor climatic conditions such as sand, dirt, humidity, moisture and snow. As per research findings from Firth *et al.* (2010), it was reported that the total yearly energy loss due to variety of faults in solar PV modules can climb as high as 18.9% ((Firth *et al*., 2010). Thus, fault detection and analysis are crucial in the quest to improve solar PV modules performance.

Parameters that are responsible for faults in a solar module are the photocurrent, series resistance, shunt resistance, saturation current density, and ideality factor (AlHajri *et al*., 2012; Chegaar *et al*., 2006; Bouzidi *et al*., 2012;). These so-called solar cell parameters are crucial

because they give deeper insights about the health of solar PV modules. In other words, faults in solar cells or modules are a reflection of abnormality with the aforementioned parameters. This research will use a simple method to evaluate four of these parameters, namely the series resistance, shunt resistance, saturation current density, and the ideality factor.

The best approach for evaluating solar modules or cells parameters is by analyzing its current-voltage curves. Hence, solar modules current/voltage curves are vital for estimating solar module parameters and carrying out fault detection and analysis. The shape of the current/voltage curves of solar modules can reveal valuable information about internal faults within the module. Researchers and engineers use solar current/voltage tracers or testers to measure and display the current-voltage curves of solar PV modules or cells.

This research involved both indoor and outdoor current/voltage measurements of solar modules using two (2) sophisticated commercial current/voltage tester and one low-cost current/voltage tester developed at the Institute for Photovoltaics(ipv), University of Stuttgart, Germany. The obtained current and voltage data were used to evaluate the solar module parameters to decipher the merits and demerits of each instrument.

1.2 Statement of the problems

Harnessing solar energy for human use involves, practically, the deployment of solar panels or modules outdoor to convert solar energy into electricity. Nowadays, millions of solar modules are being produced worldwide to serve this purpose.

However, due to physical climatic conditions, the performance of outdoor installed solar modules decrease over time. There are five (5) critical parameters whose alterations lead to faults in solar PV modules (Ali *et al.*, 2017). Evaluating theses parameters is pivoted in helping engineers, researchers and even local installers to improve solar cell or modules designs, enhance manufacturing processes, and optimize overall system performance. Hence, several researches have been done over the past decades and myriads of techniques and methods have been developed to estimate solar cell parameters (Aberle *et al.*, 2011; AlHajri *et al.*, 2012; Teyabeen *et al.*, 2020; Yauri & Espino, 2023; Agarwal *et al.*, 1981; Cholish *et al.*, 2019; Khunchan & Wiengmoon, 2018; Chegaar *et al.*, 2004; Isdawimah *et al.*, 2019; Cubas & Pindado, 2014; Yaqoob & Obed, 2019). Most of these techniques and methods involve either an analytical approach or a graphical manipulation of the current-voltage curves of the solar module or cell to extract the parameters of interest. This makes solar module current/voltage

curves measurement a crucial and foremost feature in evaluating solar module parameters. Solar module current/voltage curve is a subject that is under intensive research, owing to the fact that important information relating to the health of the solar module are embedded into the current/voltage graph (Mellit *et al*., 2018).

The instruments that are used to measure and graphically display the current/voltage curves of solar modules or cells are known as solar current/voltage tracers or testers. Commercial current/voltage tracers are convenient and widely used instruments in measuring solar PV current/voltage curves and can be obtained from different manufacturers (Hiscocks & Gaston, 2007). Their parts include the power source, the switches and the x- and y-axes for displaying the current/voltage curve. While commercial current/voltage tracers are suitable to use for current/voltage measurements, their exorbitant cost and huge size present a disadvantage for institutions and researchers with low incomes (Isaac Morko Kwembur, 2013). Consequently, new researches have been done to devised low cost I-V tracers(Cáceres *et al*., 2020; Das, 2016, 2016; Hiscocks & Gaston, 2007; Kongphet *et al.*, 2022; Leite *et al*., 2012.). However, concerns have been raised about the reliability and precision of low-cost current/voltage tracers compared to their sophisticated counterparts. Despite the importance of both I-V tracers, no comprehensive and methodical research has been conducted to compare their accuracy and reliability in measuring solar modules I-V curves; hence, this work aims to help fill this gap.

Furthermore, employing current/voltage curve tracers to measure the current/voltage curves of solar module is the primary step in extracting solar cell parameters. After measuring an I-V curve with a current/voltage tracer, a suitable evaluation method is applied to obtain the parameters of interest. Though many researchers have made great strides in the pursuit of methods to obtained solar module parameters from their current voltage curves; nevertheless, many of the methods proposed in the literature involve either complicated mathematics or cumbersome graphical analysis(Agarwal *et al*., 1981; Bai *et al*., 2014; Cubas & Pindado, 2014; Khunchan & Wiengmoon, 2018). In addition, some of the results obtained using these methods have proven to be inconsistent. Therefore, the need to employ a simple but accurate method to evaluate solar cell parameters is imperative.

1.3 Objectives

The main objective of this research is to carry out a comprehensive and systematic comparison between commercial and low-cost solar Photovoltaics current/voltage testers by determining their reliability and accuracy in measuring current/voltage curves and evaluating solar cell and module parameters.

1.3.1 Specific Objectives

1. To employ a simple but accurate method for evaluating solar cell/module current/voltage curves.
2. To determine the series resistance, shunt resistance, saturation current density, and ideality factor of solar cell and modules.
3. To compare low-cost and commercial solar current/voltage testers in order to provide insights and help decipher the merits and demerits of each type of instrument.

1.3.2 Research Questions

1. How reliable and accurate are commercial current/voltage tracers and how do they compare?
2. How accurate and reliable is a low-cost tracer when compared to its commercial counterpart?
3. How accurate is the Werner method is estimating solar modules/cells parameters?

Chapter 2: Literature review

2.1 Introduction

The measurement of the current/voltage curves of solar modules can be executed using variety of methods. These methods are based on the type of electrical load used and are utilized in the development and operation of solar module current/voltage testers. The most commonly used of these methods include resistive load, capacitive load, electronic load, DC-DC converter method and the four-quadrant power supply method. The merits of each method depends on the speed, repeatability, the number of measurements, and how easy the measuring system can be used (Duran et al., 2008). This chapter reviews the most commonly used methods to measure and display solar module current/voltage curves.

2.2.1 Resistive load method

The resistive load method is the simplest and most common used method in the measurement of solar module I-V curves. In this method, a variable resistor R of known resistance is connected in series with a solar module as shown in fig. 2.1.
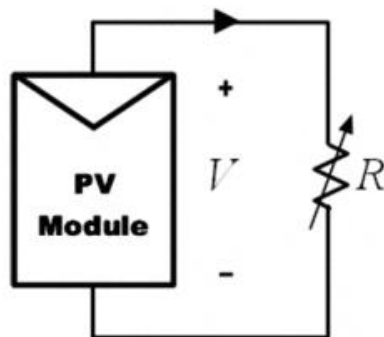
Figure 2.1 Resistive load method for solar module I-V measurement (Duran et al., 2008)

The variable resistor is increased manually from zero to infinity while the current and voltage points are displayed on a digital multimeter and recorded with each increment. This method does not require any sophisticated or complicated setup or knowledge for operation. It is simple, direct and cost-effective. Despite these merits, the resistive load method has several drawbacks. It was reported in (Mahmoud, 2006) that a manual adjustment of the load resistor can significantly slow the measurement process, introducing errors in the irradiation and temperature readings. To avoid the manual adjustment of the load resistor, Van Dyk et al. (2005) used a computer and a set of relays to acquire specific resistor value. Using this approach, the data acquisition was done efficiently compared to what is achieved when using

manual adjustment. Other drawbacks of this method include the inability to precisely determine the short circuit current point, labor requirement, and the lack of high power and wide range of resistors on the market.

2.1.2 Capacitive load method

Unlike the resistive load method that uses a variable resistor as the load, the capacitive load method uses a capacitor as its load. The most essential parts of instruments that employ the capacitive load method are the switch, the data acquisition system, the capacitor, sensor, and the controlled system. Figure 2.2 shows a simplified, schematic diagram of the capacitive load method for measuring solar module I-V curves.
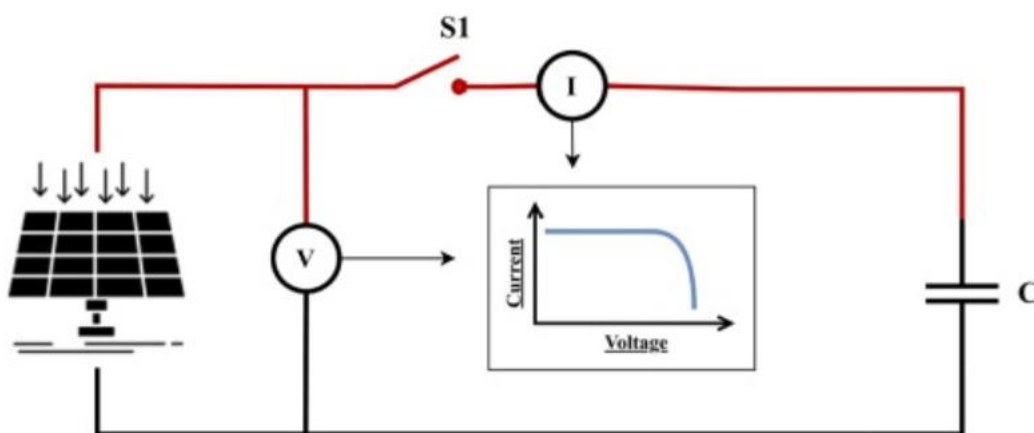
Figure 2.2 Capacitive load scheme (Londoño et al., 2022)

In fig. 2.2, the solar module is directly connected to the capacitor C. Initially, When the switch S1 is closed, the dc voltage of the solar module begins to charge the capacitor C, leading to an increase in the charge of the capacitor consequently increasing in current of the module while decreasing the voltage. The current and voltage values are read by the current and voltage sensors V and I respectively. At the end of the charging process, the supplied current becomes zero, leading to short circuit condition. This method leads to a buildup of charges inside of the capacitor until it exceeds the threshold of the open circuit voltage, at which time the I-V data points are captured. When using this method, capacitors of very good quality are desirable in order to obtain a reliable I-V curve (Duran et al., 2008). In other cases, more than one switches are used to improve the quality of the measurement. The capacitive load method is accurate and economical and is widely used in commercial I-V testers (Pereira et al., 2021).

2.1.3 Electronic load method

Figure 2.3 shows the circuitry of the electronic load method. In this figure, the load used is a transistor, particular a metal oxide semiconductor field effect transistor (MOSFET). R_S, V_{GS}, I_D, V_{DS} represent the drain-source resistance, the gate source voltage, the drain current and the drain-source voltage of the MOSFET respectively while V_{PV} and I_{PV} are the voltage and current of the solar module. In the schematics, the MOSFET is used in place of a resistor or capacitor to vary the load on the module and observe the response. This is done by adjusting the gate-source voltage V_{GS} of the MOSFET over a range of values while measuring the current and voltage of the solar module. The gate-source voltage V_{GS} helps to control the conductivity at the terminals of the Pulse width modulator (PWM) and the MOSFET.
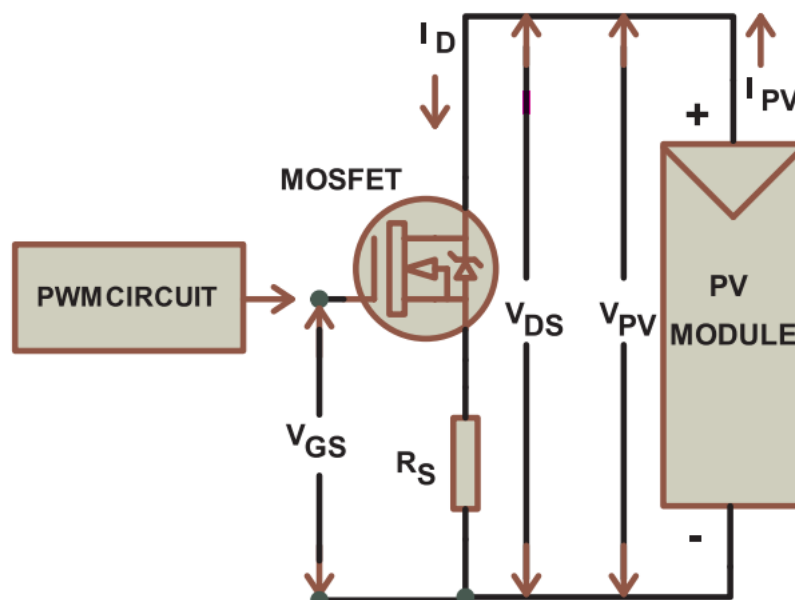
Figure 2.3 Schematics of the Electronic load method (Willoughby & Osinowo, 2018)

The MOSFET operates by applying voltage to the gate terminal, which creates an electric field that controls the flow of current between the source and the drain terminals. The resistance lies between the drain and the source and is known as the drain-source resistance R_S. The fluctuation in the resistance R_S between the drain and source caused by the gate-source voltage adjustment governs the magnitude of current obtained from the module. In order to accurately measure the I-V curve, the MOSFET must work in all states of operation, namely cut-off, active and ohmic regions. As its advantage, the electronic load method controls wide range of current and voltage, has low on-state resistance, fast switching time, and low thermal resistance. As a drawback, the electronic load controls the power degenerated by the solar module, which can

limit the application of the electronic load method to medium power(Willoughby & Osinowo, 2018). Furthermore, the electronic load method can sweep the I-V curves measurement in any direction, from open circuit voltage to short circuit current and vice versa. Also, due to the load used, some of the power produced by the module can be dissipated into heat during the measurement; therefore, the safe operation of this method both requires a cooling system and a heat sink to captured the heat produced during measurement.

2.1.4 Four-quadrant power supply method

Figure 2.4 gives an illustration of the four-quadrant power supply method for measuring the current/voltage curve of solar modules. This method can measure both positive and negative voltages and current of solar modules during testing, enabling operation in quadrant I, II, III, or IV. Many current/voltage testers normally use the 2-quadrant method to measure and display solar module current/voltage curve.
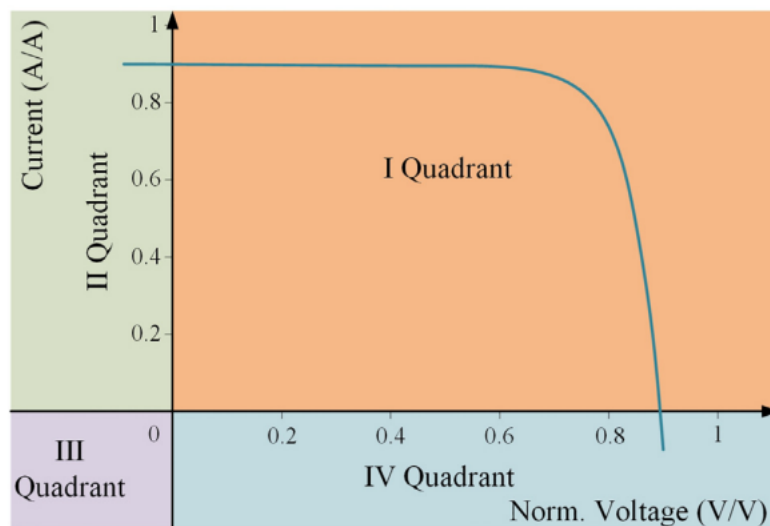
Figure 2.4 Current/voltage measured using the 4-quadrant power supply method (Zhu & Xiao, 2020)

Such instruments can measure the current/voltage curves of solar modules in quadrant I and quadrant IV, where the module acts as current source and current sink respectively. However, the most advanced solar PV testers on the market measure current/voltage curves using the 4-quadrant method. Beyond solar module characterization which usually happens in quadrant I & IV, quadrant II and III are important for identifying faults caused by mismatch of the modules (Duran et al., 2008). This method is used by researchers to demonstrate real world load scenarios.

Figure 2.5 is a simple schematic of the 4-quadrant power supply method. The PV module connects directly to a four-quadrant power supply controlled by the monitor or controlled
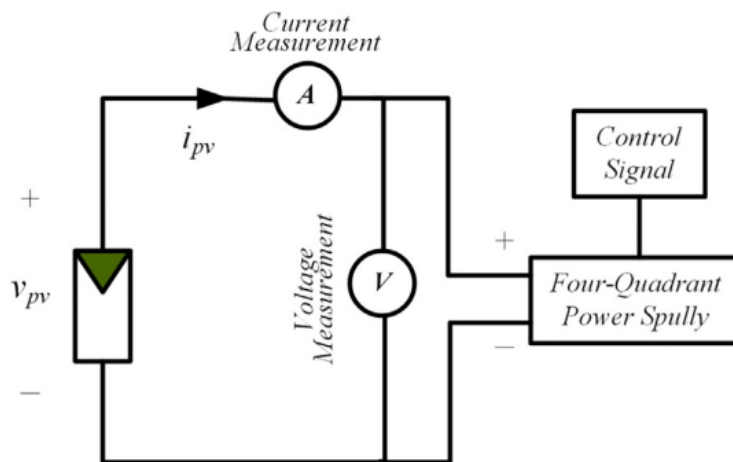
Figure 2.5 Basic setup for the four-quadrant power supply method for I-V measurement

signal. A microcontroller and microprocessor can be used to perform and automatic voltage sweep. As the sweep is done, the voltage and current readings are detected by the current and voltage sensors A and B.

Because of its sophistication, the four quadrant power supply method is the best I-V measurement method in terms of its speed and accuracy (Zhu & Xiao, 2020). Furthermore, it can measure up to 1000V and 100A. However, the four-quadrant power supply method is very cost-intensive and takes more space for measurement and measures only one PV module at a time. Hence, its application is restricted to indoor or laboratory measurement.

2.1.4 DC-DC load method

Figure 2.6 shows the diagram for DC-DC load method. The out current and voltage I & V from the solar module are regulated by the DC-DC converter. The chopper or DC-DC converter convert works by rapidly turning the DC input voltage on and off in a controlled way to produce a pulsed DC output voltage. The interval between the ON and Off switching is known as the duty cycle.
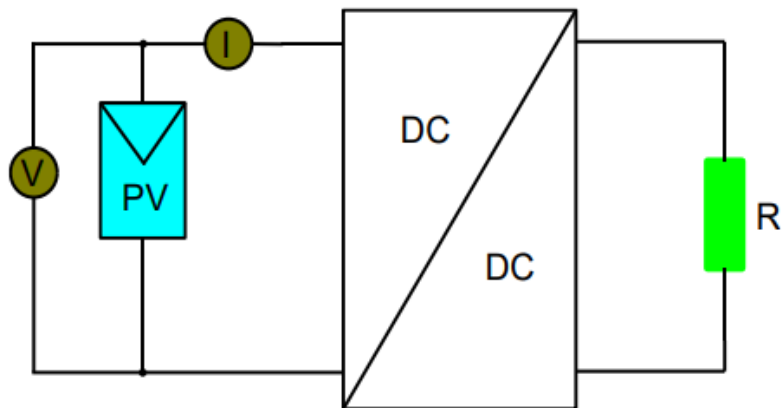
Figure 2.6. Schematics of the DC-DC load method for measuring current/voltage curve

The DC-DC load method is principally based on three (3) configurations, namely boost converter, buck converter and buck-boost converter. Using an electrically generated Paulse Width Modulation (PWM) signal with a uniform frequency and variable duty cycle (D) ranging from 0 to 1, a DC-DC converter can transform the amplitude of the DC voltage up or down and/or reverse the polarity(Sayyad & Nasikkar, 2021). The DC-DC converter method is one of the most efficient and low cost method for tracing I-V curves and has been used by several researchers to develop low cost I-V tracers(Duran et al., 2008; Durán et al., 2012; Enrique et al., 2005; Khatib et al., 2017; Pereira et al., 2021). It has several advantages over other current/voltage tracing methods on the market in terms of modularity, speed, flexibility, direct display and cost.

Table 2.1. A summary and comparison of all reviewed current/voltage curves measurement methods.

Method	Modularity	Fidelity	Fast Response	Flexibility	Direct Display	Cost
Variable Resistor	Medium	Medium	Medium	Low	No	Low
Capacitive Load	Low	Low	Medium	Low	No	High
Electronic Load	High	High	Medium	Medium	Yes	High
Four quadrant power supply	Low	Low	High	High	No	High
DC-DC load	High	High	High	High	Yes	Low

Chapter 3: Theoretical background

Solar energy can be defined as the radiant energy from the sun which can be transformed into usable forms such as electricity and heat. The direct transformation of solar energy into electricity is known as photovoltaics. This chapter introduces the principles of photovoltaics, explains the operations of solar cell and diodes, as well as defines key parameters that are used in characterizing solar cells/modules.

3.1 Working principle of a solar cell

A solar cell or a photovoltaic cell is an electrical device that converts solar energy into electrical energy. PV modules are manufactured by connecting several solar cells either in series or parallel. Series connection of solar cells increases the voltage output of the module while parallel connection increases the current output.
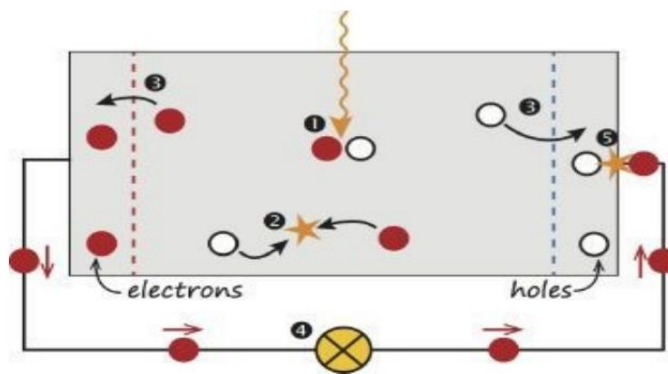
Figure 3.1. Model of a solar cell. 1. Absorption of a photon leads to the generation of an electron hole pair. 2. Usually, the electrons and holes will recombine. 3. With semipermeable membranes the electrons and the holes can be separated. 4. The separated electrons can be used to drive an electric circuit. 5. After the electrons have passed through the circuit, they will recombine with holes. (Smets et al., 2016)

Solar cells convert solar energy into electricity through a phenomenon known as photovoltaic effect. The photovoltaic effect is a phenomenon that involves the generation of voltage or current when a semiconducting material is exposed to sunlight. It is governed by the generation of charge carriers as a result of photon absorption, the subsequent separation of the photo-generated charge carriers, and the collection of photo-generated charge carriers.

3.1.1 The current/voltage characteristics of a solar module
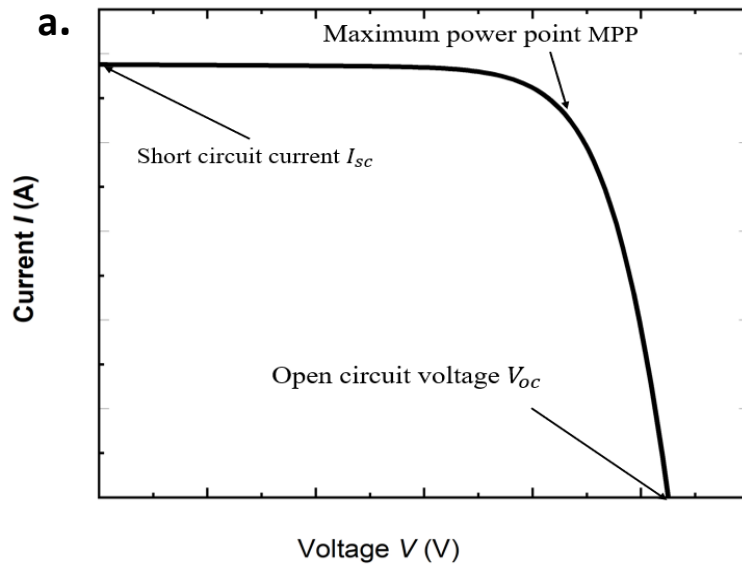
Figure 3.2. a.) Typical current/voltage curve of a solar module in quadrant I
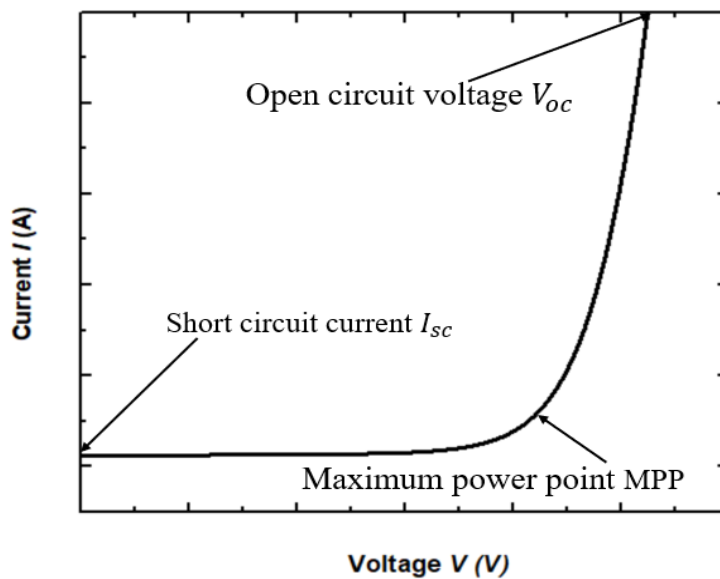
Figure 3.2. b.) Typical current/voltage curve of a solar module in quadrant I

The current-voltage curve of a solar module depicts the graphical representation of the current and the voltage variation of the solar module when under operation. Fig. 3.2a and 3.2b. depict the shapes of typical solar cell or module current/voltage curves displayed in quadrant I and

quadrant IV of the x-y plane. In quadrant I, both the current and the voltage out of the solar module or solar cell are positive-positive while in quadrant IV, the current produced is negative and the voltage is positive. case. The main points on a solar module current/voltage curve are the short circuit current I_{SC}, the open circuit voltage V_{OC}, and the maximum power MPP.

3.1.2   Solar module electrical parameters

3.1.2.1 Open circuit voltage V_{OC}

The open circuit voltage of a solar PV module is the voltage at which the current produced by the PV module is zero. The I-V curve intercepts the x-axis (the voltage axis) at the open circuit voltage as shown in figure 3.2 a. and 3.2 b. The open circuit voltage is significantly affected by temperature. An increase in the temperature of the module decreases the open circuit voltage and the maximum power point. The open circuit voltage is related to temperature, short circuit current density and saturation current density by

$$V_{OC} = k_B T/q \ln(J_{SC}/J_O + 1),\qquad(1)$$

where T represents the absolute temperature; J_{SC} is the short circuit current density, J_O is the saturation current density and k_B and q are the Boltzmann constant and the electron charge equal to $8.62\times 10^{-15} eV/K$ and $1.60 \times 10^{-19} As$ respectively.

3.1.2.2 Short circuit current and short circuit current density

The short circuit current is the maximum current flowing in a solar module when the voltage drop across the terminal is zero. The short circuit current is indicated at the point of interception of the y-axis (the current axis) on the solar I-V curve as shown in figure 3.2 a. and 3.2b. Because the short circuit current depends on the area of a solar cell, it has to be divided by the area when comparing different solar cell. This area normalized short circuit current is known as short circuit current density J_{SC}. It is an important parameter when comparing different solar cell or module as it allows the standard measure of the short circuit current regardless the sizes of the cell.

3.1.2.3 The maximum power point MPP

The maximum power point is the point on the solar cell or module I-V curve where the product of the current and voltage is maximum. This point is vital in terms of harnessing the maximum efficiency of the solar module. A decrease in the maximum power point results to a decrease in the efficiency and fill factor of the solar module.

3.1.3 The single diode model and equivalent circuit of a solar cell

Figure 3.3 illustrates the equivalent circuit of the single diode model of a solar cell. In the diagram, I_{ph} represents the photocurrent; I_d is the current passing through the diode; R_S and R_P are the series resistance and parallel resistance respective while I and V are the output current and voltage of the solar cell measured at the terminals. These elements collectively contribute to the performance of the solar cell under specific operational conditions.

The single diode model, which main feature is a diode connected in parallel with a photocurrent, is the simplest model used to depict the circuit of a solar cell. As shown in fig. 3.3, it consists of four key parameters (i.e I_{ph}, I_d, R_S, R_P) that are properties of the diode. Besides this model, other models such as the double diode and the triple diode models exist, but are very complex in nature. As a result, the single diode model was used in this work to ensure a non-complicated and direct approach for analyzing the cell and module parameters.
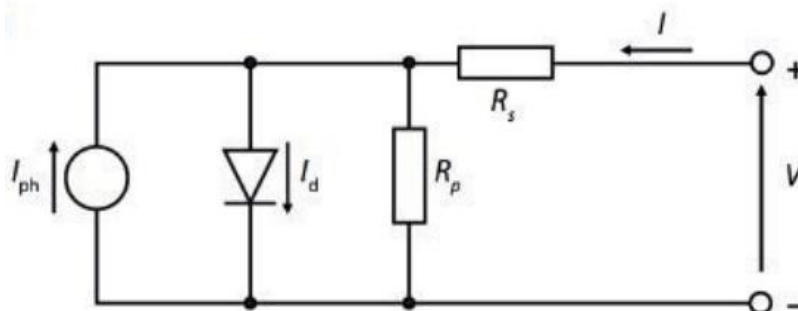
Figure 3.3. Equivalent circuit of the single diode model of a solar cell (Smets et al., 2016)

Equations (2) to (4) describe the equations for a solar cell for different conditions. Equation 2 assumes that the solar cell is ideal and operates in the dark; hence, there is no effect of series

$$J = J_0 \left(\exp\left(\frac{qV}{nkT}\right) - 1\right) \tag{2}$$

$$J = J_0 \left(\exp\left(\frac{qV}{nkT}\right) - 1\right) - J_{sc} \tag{3}$$

$$J = J_0 \left(\exp\left(q\left(\frac{V-IR_s}{nkT}\right) - 1\right) + \left(\frac{V-IR_s}{R_p}\right) - J_{sc}\right. \tag{4}$$

resistance, parallel resistance and photocurrent in this case. In fact, for an ideal solar cell, the photocurrent I_{ph} is the same as the short circuit current density J_{sc}. However, for series resistance larger than 10 $\Omega\,cm^2$, the short circuit current density J_{sc} becomes less than the photocurrent density J_{ph}. In this case, the short circuit current density can be approximated by

$$J_{sc} = J_{ph}\frac{R_p}{R_p + R_s} \,. \tag{5}$$

Unlike eq. (2) that represents a solar cell that operates in the dark, eq. (3) represents a solar cell that is illuminated. Equation (4) represents a real solar cell under illumination with the effect of both series and parallel resistance.

3.2 Solar module/cell parameters extraction and the Werner evaluation method

The fundamental function of any solar cell or module is to efficiently convert solar energy into electrical energy. However, the performance of solar modules hinges on key parameters, namely, photocurrent, series resistance, shunt resistance, saturation current, and ideality factor (AlHajri et al., 2012; Bouzidi et al., 2012; Chegaar et al., 2006). The extraction and estimation of theses parameters provide vital information on the device's performance, efficiency, and potential areas for development. Accurate evaluation allows researchers, engineers, local installers, and manufacturers to improve solar cell designs, enhance manufacturing processes, and optimize overall system performance. Nevertheless, due to the nonlinear, implicit characteristics of eq.(4), the extraction of solar cell parameters has proven to be a herculean task.

This section introduces a classical method known as the Werner evaluation method or the Werner plots to extract essential solar cell or module parameters. The Werner evaluation method is a simplified and straightforward method to extract diode or solar cell parameters without employing complex mathematical models or complicated computer algorithms (Ouennoughi & Chegaar, 1999; Werner, 1988). The application of this method allows the

extraction of critical solar cell parameters with high accuracy and helps researchers, engineers, and local installers to gain deeper insights into the performance of solar modules. Its robust approach encompasses the utilization of solar cell I-V curves, simple mathematical models and curve fitting techniques to access essential solar cell parameters. Having introduced the basic principles of Werner's method, I will proceed to delve into its derivation and explore its significance using different plots.

3.2. 1 Derivation of Werner evaluation method

For $R_p = \infty$, and $J_{ph} = J_{sc}$, eq. (4). reduces to

$$J = (J_o e^{\frac{q(V-JR_S)}{nkT}} - 1) - J_{sc}. \tag{6}$$

Equation (6) begins the derivation of the Werner evaluation method.

To begin with, J_{sc} is transferred to the left-hand side (LHS) of the eq. (6) and the derivative of the current is taken with respect to the voltage to yield:

$$\frac{d(J+J_{sc})}{dV} = (J_o e^{\frac{q(V-JR_S)}{nKT}} - 1) \frac{q}{nKT} (1 - \frac{dJ}{dV} R_s), \tag{7}$$

Where all symbols maintain their usual definitions.

Let $J_d = J + J_{sc} = (J_o e^{\frac{q(V-JR_S)}{nKT}} - 1)$ and $\frac{dJ}{dV} = G$, where J_d *and* G represent the diode current and conductance respectively.

Substituting J_d *and* G into eq. (6) gives

$$\frac{G}{J_d} = (\frac{q}{nKT}) (1 - GR_s) \tag{8}$$

Equation (7) represent a linear equation with $y = G/J_d$ and $x = G$. This gives the first method for determining the series resistance R_s and ideality factor n_1. By fitting eq. (8) to the plot of G/J_d vs. G, the series resistance R_s and the ideality factor n_1 can be determined from the x and y intercepts of the plot respectively.

The second approach for determining the ideality factor n_2 and the saturation current density J_o of a solar cell using the Werner evaluation method is by fitting the semi log plot of the dark J-V curve. The series resistance is then determined by fitting the plot at the region where series

resistance dominates (the region of higher voltages) while the saturation current density is given by the y-intercept of the plot.

The third method for determining the ideality factor n_3 using the Werner Evaluation method is derived below:

At open circuit condition, $J = 0$, and $G_{oc} = G|_{J=0}$.

Where G_{oc} = conductance at open circuit condition. Substituting into eq.(8) yields

$$G_{oc} = J_{sc}\frac{q}{nKT}(1- G_{oc}R_s) \tag{9}$$

From eq. (9), the goal is to determine the resistance at open circuit condition R_{oc}. Since resistance is the reciprocal of conductance; hence,

$$R_{oc} = \frac{1}{G_{oc}} = R_s + \frac{nkT}{J_{sc}q}; \quad \text{i.e} \qquad R_{oc} = R_s + \frac{nkT}{J_{sc}q} \tag{10}$$

Equation (10) shows that the resistance of a solar cell at open circuit condition R_{oc} is greater than the actual series resistance of the cell R_s by a factor of $nkT/(J_{sc}q)$.

This proof implies that it is erroneous to determine the series resistance of a solar cell by taking the slope of the I-V curve at open circuit condition.

Further, the third method for determining ideality factor n_3 and series resistance R_s via the Werner plot is by fitting eq.(10) to the plot of R_{oc} *vs.* J_{SC}^{-1} *and then* taking the slope and y-intercept of the plot. The slope of the plot gives the ideality factor while the y-intercept give the series resistance.

Equation 6 to 10 demonstrate the mathematical derivation of the Werner evaluation method. To appreciate this method, first, several plots are used to demonstrate via graphical and numerical approaches the effects and implications of solar cell parameters on the current/voltage curves. Second, the Werner method is used to illustrate how these parameters are obtained.

Consider the dark current/voltage plots of nine (9) different theoretical solar cells shown in fig.10. Notice that the plots are on a semi-log scale with every plot having the same ideality factor converging to a common point in groups of three (3). This common point of convergence is the open circuit voltage of the cells. Because the solar cells are in the dark with no effect of

series and shunt resistances, and their J-V curves are in semilog forms, the equation governing any of the curves takes the form,

$$lnJ = lnJ_o + \frac{q}{nkT}V \tag{11}$$

where, q/nkT represent the slope lnJ_o represent the y-intercept.

Thus, eq. (10) demonstrates how the ideality factor and saturation current density are determined from the given plots.
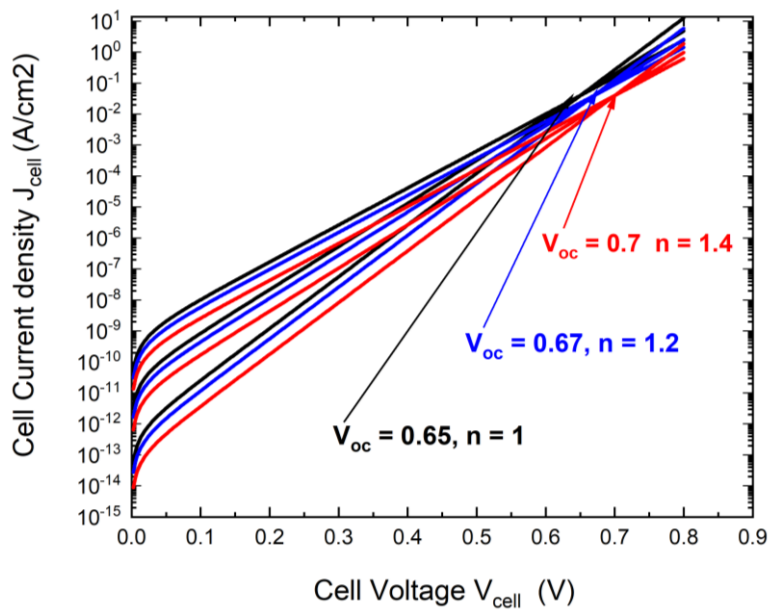
Figure 3.4. Semi log plots of the current/ voltage curves for 9 theoretical solar cells. Cells with the same ideality factor converge to a common point (at the same open circuit voltage).
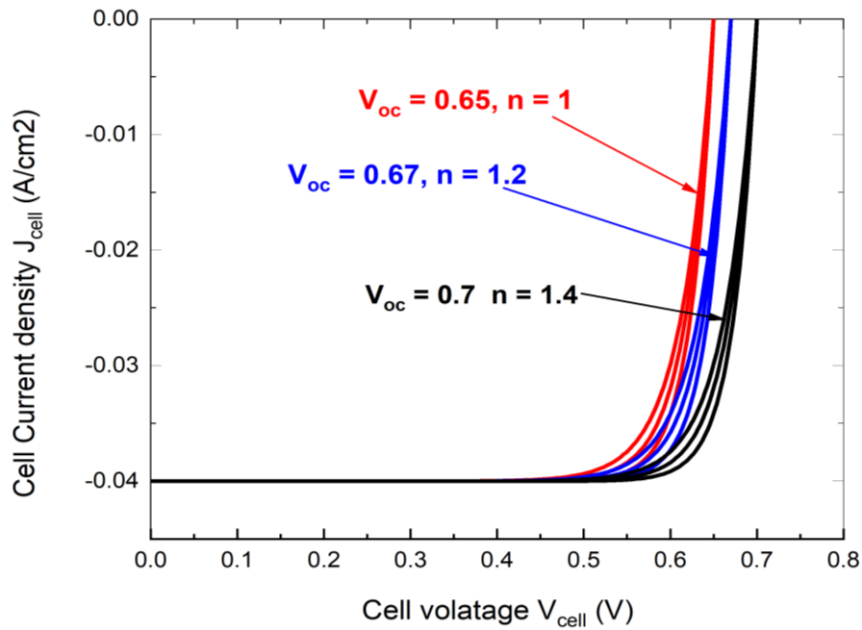
Figure 3.5. Linear scale current/ voltage plots for 9 theoretical solar cells. Cells with the same ideality factor converge to a common point (at the same open circuit voltage).

Fig 3.4 and 3.5 describe the same solar cell current/voltage curves, but plotted on semilogarithmic and linear scales respectively. For both figures, increasing in the ideality factor shifts the plots towards higher voltages with plots having the same ideality factor meeting at the same open circuit voltage.
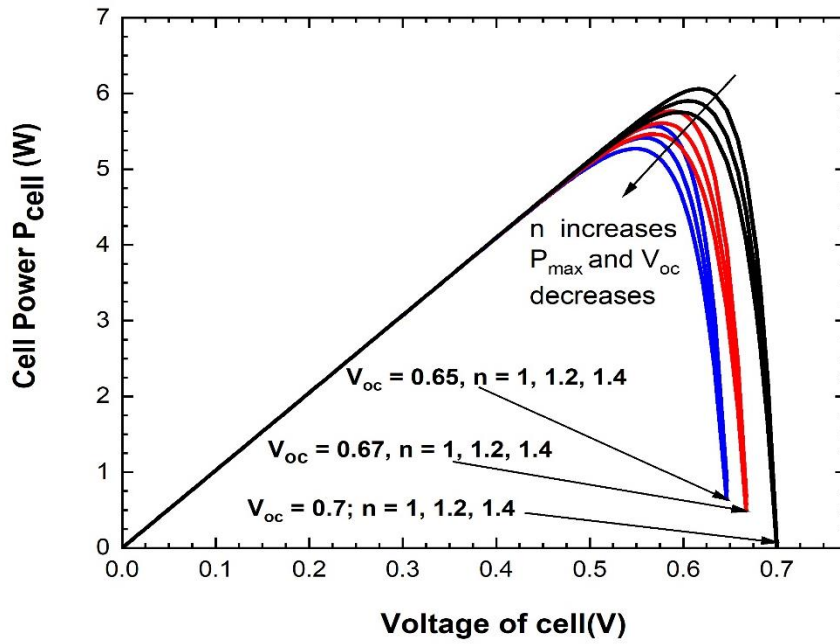
Figure 3.6. Power/ voltage curves for the 9 different illuminated solar cells in figure 3. Cells with the same ideality factor converge to a common point (at the same open circuit voltage).

Figure 3.6 demonstrates how the power output of solar cells is affected by ideality factor and saturation current density. Saturation current density is exponentially related to the open circuit voltage by:

$$J_o = J_{sc}(e^{-\frac{q(V_{oc})}{nKT}}) \tag{12}$$

That is, the smaller the saturation current density, the higher the open circuit and vice versa. Also, ideality factor signifies recombination losses in a solar cell. Increase in ideality factors result in higher recombination losses in a solar cell and further leads to a reduction in the open circuit voltage and maximum power point as seem in fig. 3.4 and consequently a reduction in the power output and fill factor (Smets et al., 2016). The nine (9) plots in fig. 3.4 are divided in to a group of three (3) based on similar open circuit voltage. The curves with the same open circuit voltage converge at a common point. For each group of curves, the ideality factor increases from top to bottom while saturation current density decreases with increase in ideality factor.

Table 3.1. Characterization table of the ideal solar cell in fig.2.5.

Solar cell Parameters	Magnitude
Open circuit voltage V_{oc} **[mV]**	650
Shor circuit current density J_{sc} **[mA/cm²]**	40
Fill Factor FF$_{ideal}$	0.83
Fill Factor FF from eq.(14)	0.84
Efficiency η **[%]**	21.06

Table 3.1 shows the characterization for the ideal solar cell in figure 3.5 with $V_{oc} = 0.65V \ and \ n = 1$. For this modelled solar cell, the ideal fill factor FFideal and efficiency η are higher due to the absence of series and shunt resistances. By comparison, the fill factor of the ideal solar cell obtained using eq. (13) is almost equal to that obtained using the green's formula (eq. 14), indicated by an insignificant relative deviation of about 1.2%. Hence, the fill factor for the ideal solar cell is in agreement with the Green's formula for estimating fill factor for ideal solar cells based on their open circuit voltage.

The fill factor is an important metric for evaluating the efficiency and performance of a solar cell, reflecting its overall quality. For silicon-based solar cells, which are commonly used in solar technology, the fill factor are typically in the ranges of 0.75 to 0.85 (Mertens, 2014, p. 79). Mathematically, the fill factor depends on the ratio of the Maximum power point to that of the product of the open circuit voltage and short circuit current. That is,

$$FF = \frac{P_{max}}{V_{oc} \times J_{sc}} . \tag{13}$$

 Also, for an ideal solar cell, a good estimation of the dependence of fill factor on open circuit voltage is given by [Green (1981)].

$$i.e \ FF = \frac{v_{oc} - \ln(v_{oc} + 0.72)}{v_{oc} + 1}, \tag{14}$$

where , v_{oc} is the reduced voltage and is defined as $v_{OC} = \frac{q}{nKT} V_{oc}.$
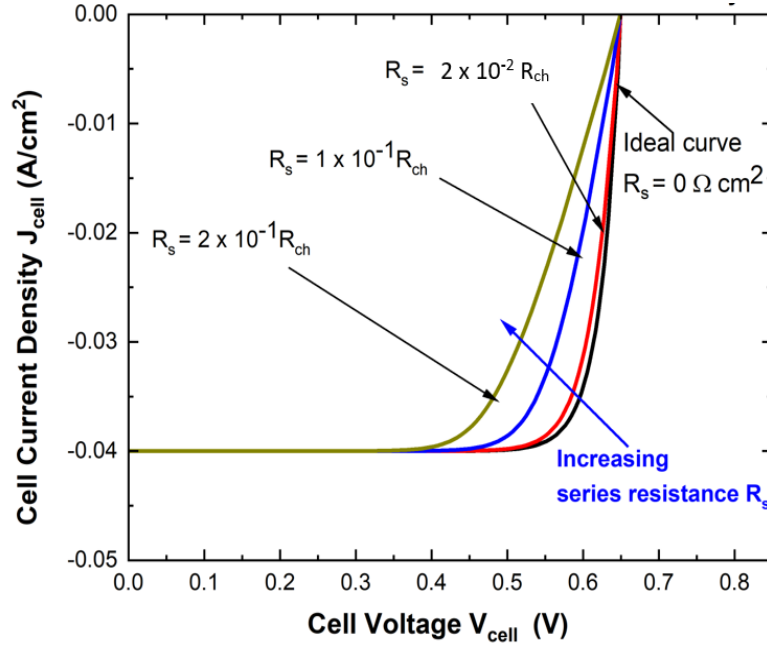
Figure 3.7. Effects of increasing series resistance of the illuminated J-V curves of solar cells. As the series resistance increases, the curves flatten inward.

On the contrary, fig. 3.7 shows that the presence of series resistances in a solar cell shrinks the I-V curves inward, affecting the position of the maximum power point. This shift in the position of the MPP leads to a decrease in the fill factor and efficiency of the cell, respectively.

The series resistances of the curves in fig. 3.7 are defined in terms of their characteristic resistances R_{ch}. The characteristic resistance R_{ch} is the ratio of the open circuit voltage to the short circuit current density. The series resistance R_s is related to the fractional power loss f and the characteristic resistance $R_{ch.}$ by:

$$R_s = f \times R_{ch},$$ (15)

where f ranges from 0 to 1 (Green, 1982).

For the plots in this work, the R_{ch} was calculated to be 16.25 Ω cm^2 and the series resistance are defined in terms of this value. As the series resistance increases in fig. 3.7, the curves flatten inward and the slope of the curves at open circuit condition becomes less steep. The ideal curve (R_s = 0) has the steepest slope and largest Fill factor and efficiency, while the curve with the highest series resistance ($R_s = 2 \times 10^{-1}$ R_{ch} has the least value of Fill Factor and efficiency.

Hence, the maximum power points, fill factors and efficiencies of the curves decrease. A summary of the effect of the series resistance on the cells parameters is given in table 3.2.

Table 3.2. Effect of series resistances on the Fill Factors FF and efficiencies of the solar cells in fig. 3.7.

Series resistance R_s [Ω cm^2]	Fill factor FF	Efficiency η [%]
0	0.83	21.06
2×10^{-2}	0.79	19.09
1×10^{-1}	0.70	18.2
2×10^{-1}	0.62	16.1

The decrease in Fill factors and efficiencies values in table 3.2 is evident by the increase in series resistance of their respective curves in fig. 3.7. Also, note that the curves in fig. 3.7 converge towards the same open circuit voltage and short circuit current density. This is so because, except for extremely large values, series resistance does not affect the position of the open circuit voltage and short circuit current density (Smets et al., 2016).
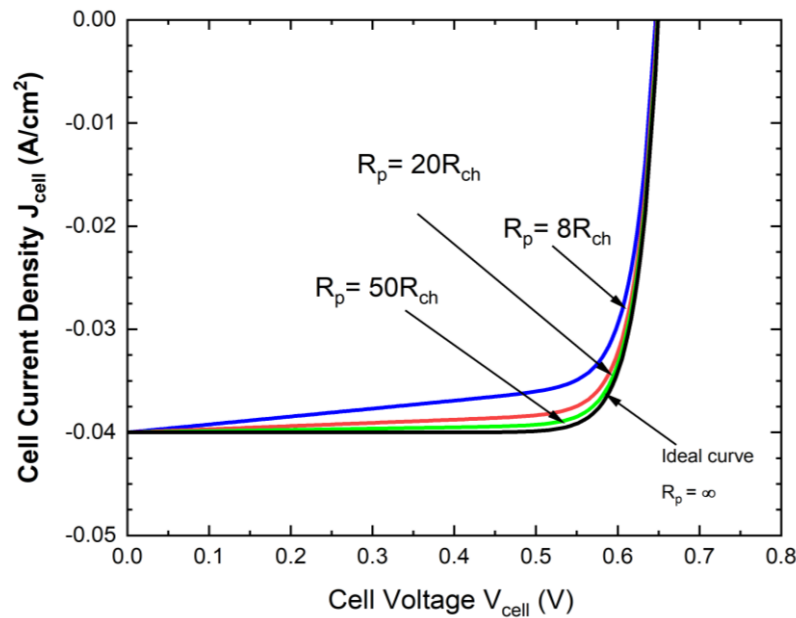
Figure 3.8. effects of decreasing shunt resistance on the current/voltage curves of solar cells. It can be observed that as the shunt resistance increases, the curves flatten inward and the position of Voc and Jsc remains the same

In fig. 3.8, the black curve represents the ideal J-V curve of the solar cell with shunt or parallel resistance of infinity. Notice that as the shunt resistance decreases, the slopes of the curves

around the short circuit current density becomes less steep and the curves deviate from ideality. Consequently, the maximum power point, the Fill factor and the efficiency are affected. In other words, a decrease in shunt resistance leads to a decrease in the fill factors and the efficiency.

Fig. 3.9 shows the ideal curve (black) and how it is affected when series resistances are added. In the figure, series resistances of different magnitudes are added to the ideal solar cell and the effect is seen by the deviations of the red, blue and green curves The greater the series resistance, the more pronounced is the deviation from the ideal curve.

Nevertheless, using the known series resistances, the affected curves can be corrected. This means, the effect of series resistance can be offset by subtracting the voltage drop due to series resistance JR_s from the cell voltage V_{cell}. The mathematical difference of the two voltages gives the voltage of the diode (i.e $V_d = V_{cell} - JR_s$).
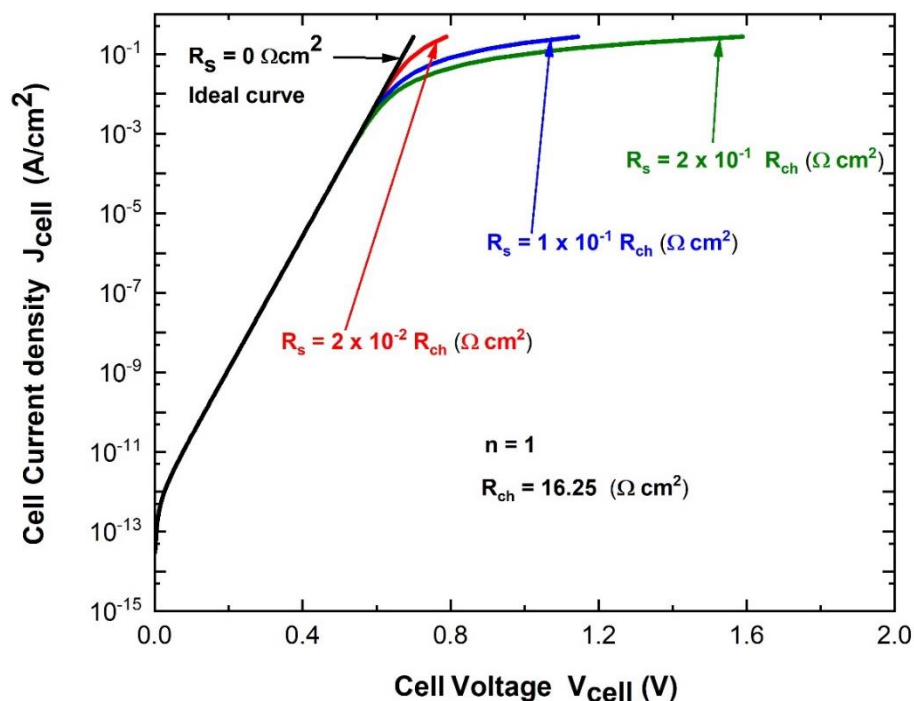
Figure3.9. Deviation of dark solar Cells J-V curves with series resistances from ideality.

Using this procedure, the red curve in fig. 13 was corrected and the result is shown in fig. 15. As expected, fig. 3.9 represents an ideal solar cell and is the same as the curve with zero resistance in fig 3.7. This corrected curve was fitted using eq.2 to demonstrate the second method for determining ideality factor n_2 and saturation current density J_o using the Werner evaluation method.
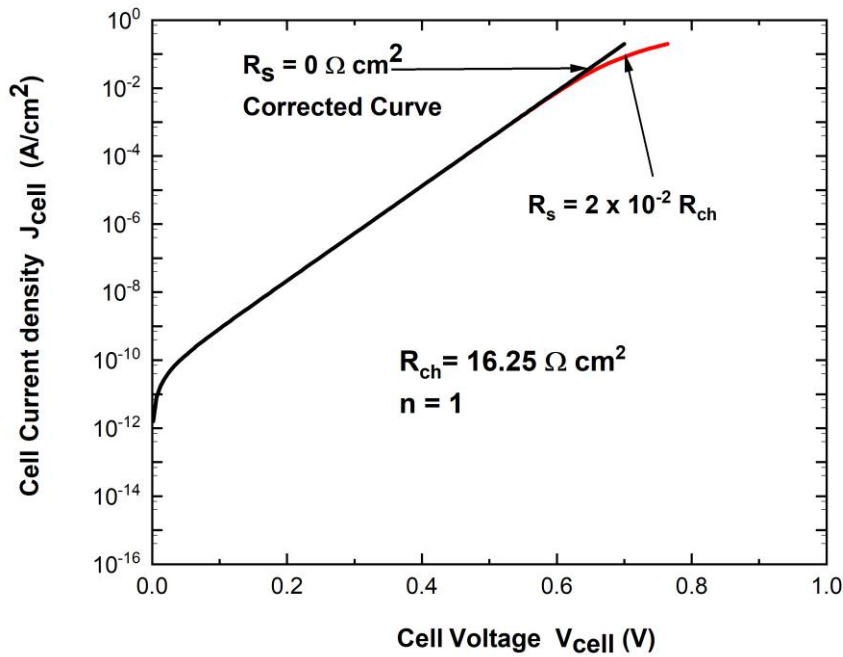
Figure 3.10. Before correction for series resistance (red curve) and after correction for series resistance (black curve)

After correcting the red curve for series resistance, it was proven, by fitting the black curve, that the ideality factor and saturation current density are n = 1 and Jo = 5.6×10^{-13} A/cm^2 respectively. When shunt resistances are added to the solar cells plots in fig. 3.9, the results are those shown in fig. 3.11.

Thus, fig 3.11 shows the effect of both series and parallel resistances on an ideal solar cell. For the non-ideal solar cells, the effects of shunt resistances are noticeable at lower voltages.
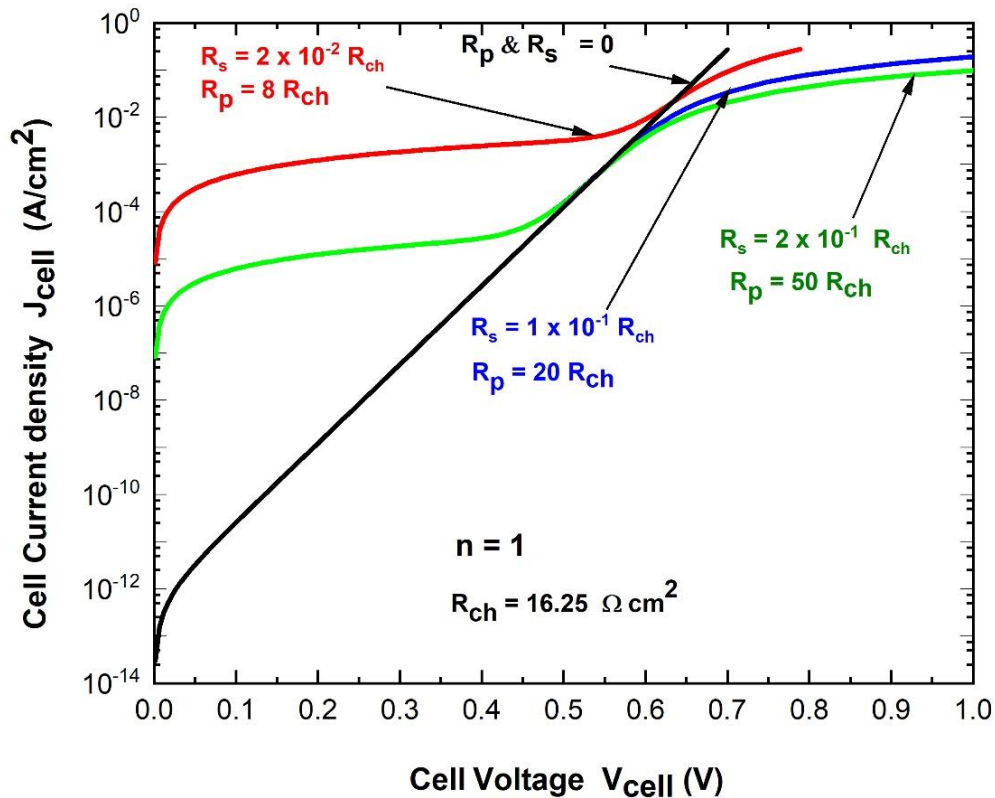
Figure 3.11. Deviation of three non-ideal solar cells with both series and parallel or shunt resistances from ideality.

However, in fig. 3.12, the series resistance is kept the same ($R_S = 2 \times 10^{-2} R_{ch}$) while the shunt resistance is varied from 8 times the characteristic resistance to 10,000 times the characteristic resistance. Thus, the plots become more linear and their maximum points slowly disappears as the shunt resistance increases. This is so because by increasing the shunt resistance, the expression $(V - IR_s)/R_p$ in equation (4) gets closer to zero. At this point, the equation of the solar cell mimic that of a diode; consequently, the plots get closer to ideality. The consequence of a very large shunt resistance in the G/Jd vs. G plot *is* clearly shown by the straight line in figure 16 (the black curve). The straight line was obtained as a result of increasing the shunt resistance to 10,000 times the characteristic resistance. As a result, the maximum point completely disappears, resulting into a linear line.
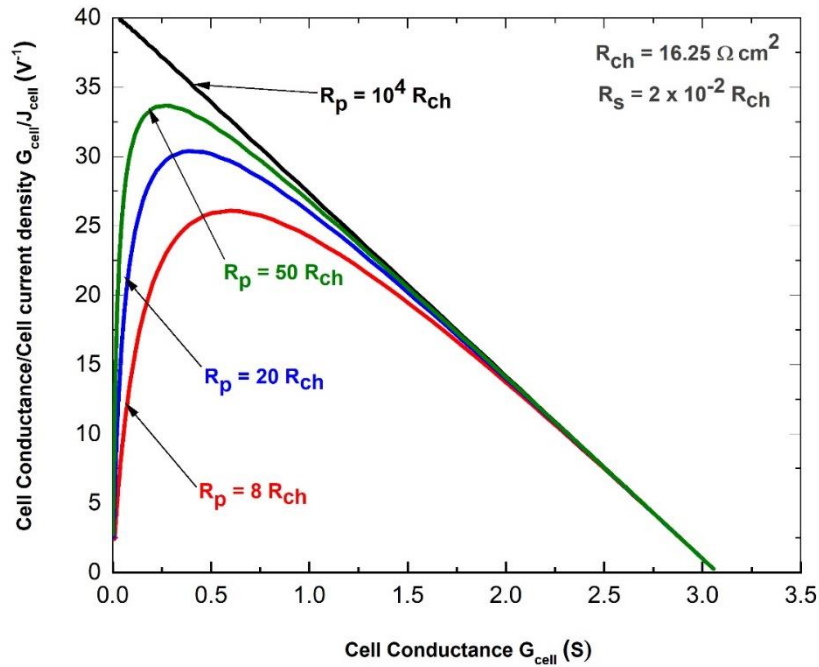
Figure 3.12. Variation of G/Jd vs. G of four solar cells with the same series resistance but different shunt resistances.

Generally, the G/Jd vs. G plots are nonlinear at lower conductance as a result of the influence of parallel resistance; but the plots become linear with increasing conductance values as a result of the influence of series resistance. Hence, the series resistance was obtained by fitting the straight line and extracting the x-intercept while the ideality factor was obtained from the y-intercept of the fitted line.
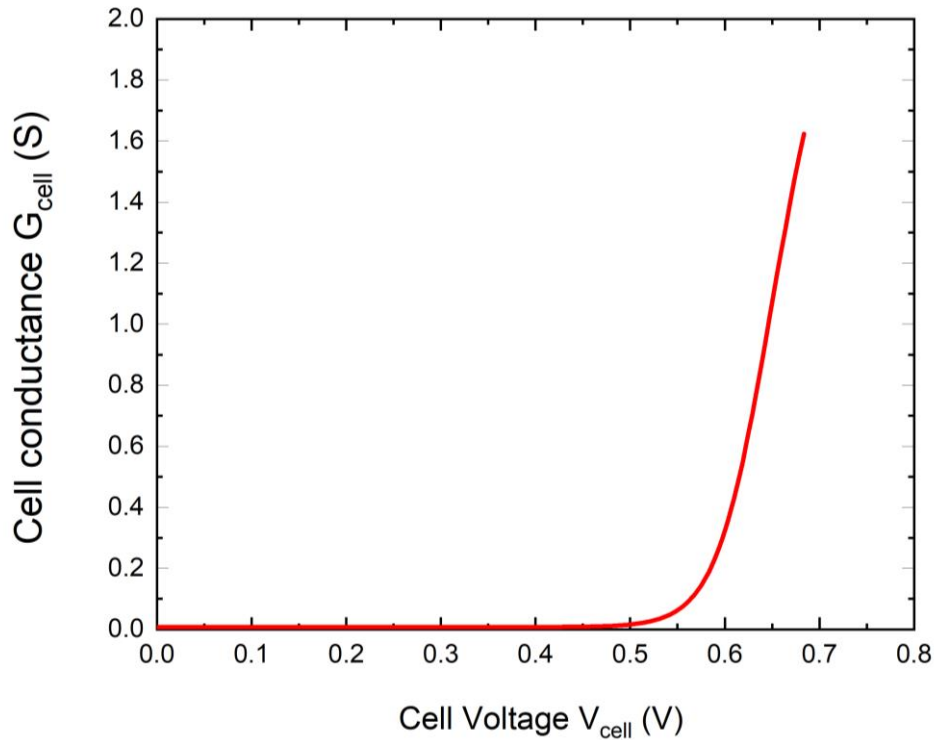
Figure 3.13. Conductance and Voltage plot of the theoretical solar cell. The conductance below 0.5V is small to be noticed on a linear scale.

Fig. 3.13 is the graph of the cell conductance vs. the cell voltage plotted on a linear scale. The curve does not rise for voltages between 0.5 volts, indicating that the cell conductance is zero in this voltage range. However, this is not true when the plot is done on a logarithmic scale. The conductance values are only very small to be detected on the linear scale. The curve will only begin to rise on the linear scale for voltages greater than 0.5V as shown in the figure.

Chapter 4: Materials and methods

This master's thesis was done at the Institute of Photovoltaics (ipv), University of Stuttgart, Germany, over the span of four (4) months. All experiments and practical works were done at the laboratories and testing facilities of the institute. This section will present the materials used for the measurements of the current-voltage data, the software used for data acquisition, as well as the methods used for data processing and analysis.

Figure 4.1a. and 4.1b. show the measurement sites. The current/voltage data were measured both indoor and outdoor. Outdoor measurements were carried out at the top floor of the institute (fig. 4.1b) where solar modules are mounted for testing while the indoor measurements were done using Wavelabs (Fig. 4.1a)
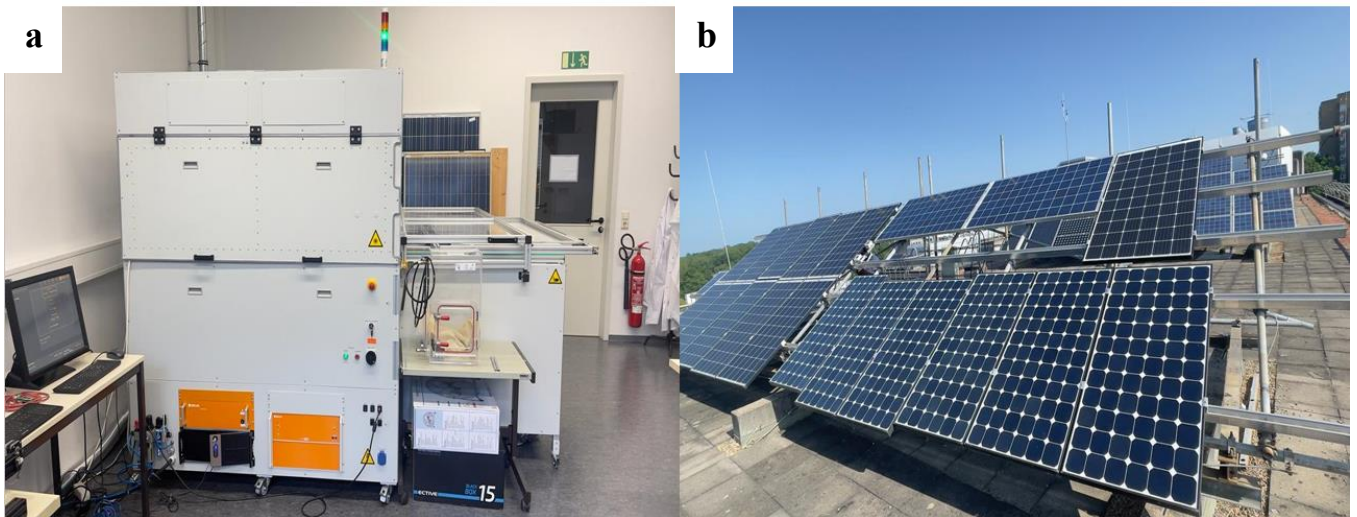
Figure 4.1. a) Indoor solar I-V testing lab and b) Outdoor mounted solar PV testing site at the Institute for Photovoltaics, University of Stuttgart.

4.1 Measurement procedure

The I-V data measurement were conducted on a total of five (5) modules. The outdoor current-voltage data were measured using the PVPM1040C commercial I-V tester and the low -cost I-V tester (ipv-Navid unit) on three (3) different monocrystalline solar modules, namely Maysun MS410MB-40H, Trina Solar TSM-400DE09.08 and Solar World Plus SW 290 Mono while the indoor measurements were conducted on the China light CLS 230P modules and the Sun Electronics SV-X-210 module.

Table 4.1. Names and characterization of measured solar modules

Name of module	Total Number of cells	V_{oc} of module [V]	V_{oc} of cell [mV]	Number of cells in series	Number of cells in parallel	J_{sc} per cell [mA/cm^2]	I_{sc} of module [A]	Area of cell [cm^2]	Efficiency of Module η [%]	Cell Technology
Maysun MS410M B-40H	80	53.24	670	80 cells in series	-	40	9.8	220.5	20.6	Half cell Heterojunction technology
Trina TSM-400DE09.08	120	40.1	690	60 cells in series	2 cells in parallel	42	12.18	147	19.9	Half cell Heterojunction technology
SolarWorld Plus Sw 290 Mono	60	39.4	670	60 cells in series	-	38	9.4	246.49	18.5	Monocrystalline Si n-type
Sun electronics SV-X-210-FA1	114	23.1	600	38 cells in series	3 cells in parallel	33	12	120	14.8	String ribbon Sovello Si p-type
Chinalight CLS-230P	60	37.38	612	60 cells series	-	35	8.3	240.3	13.2	Block cast Si p-type

Table 4.1 shows the summary characterization of the measured solar modules used in this work. The pictures of four of the modules are shown in figure 4.2 while the 5th module is shown in figure 4.3. The 5th module (SolarWorld Plus Sw 290 Mono) was already mounted and could not be removed.
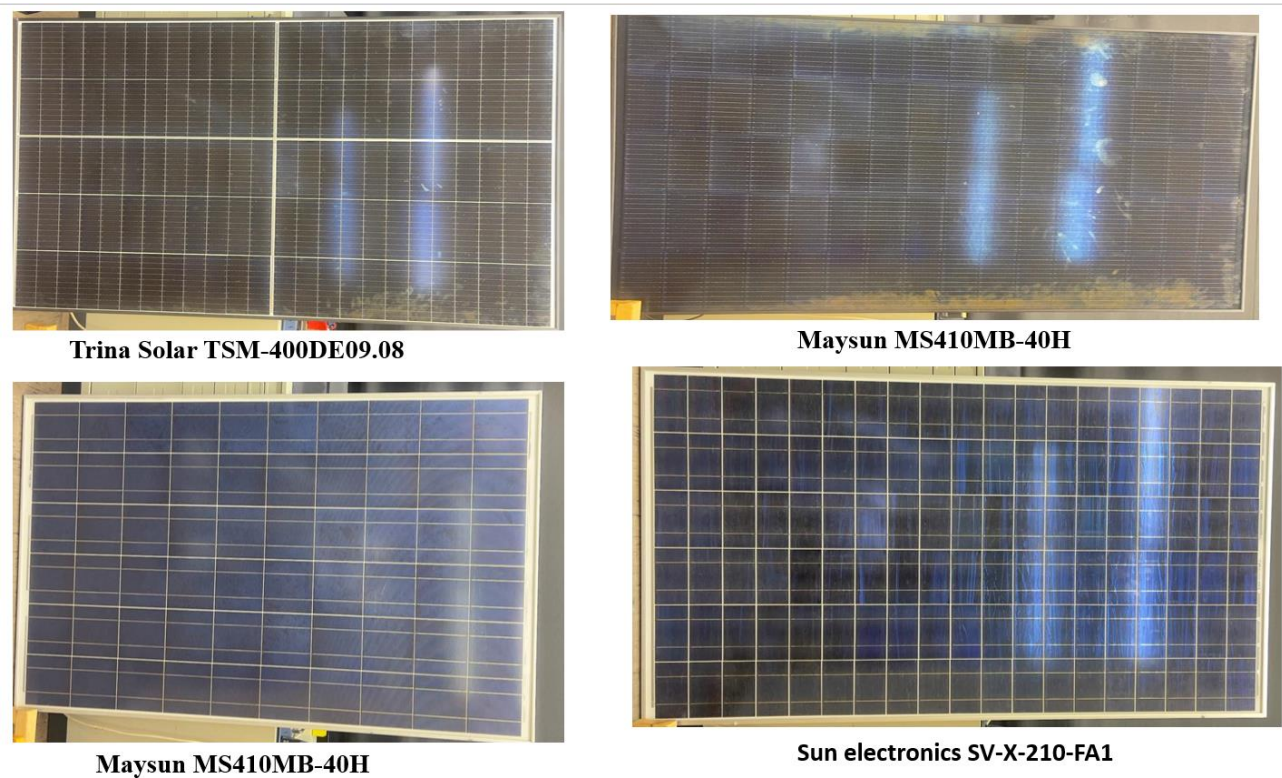
Figure 4.2. Four of the solar modules that were used for measurements

Furthermore, unlike the Triana and Maysun modules that were less than two (2) months old, the SolarWorld, China light and Sun Electronic modules had significant aging, having been used outdoor for over sixteen (16) years. Before beginning the outdoor measurements, the I-V testers were connected to their respective hardware, cables and sensors. Similarly, the solar modules were mounted and connected to their respective sensors and cables. Next, each solar module was measured with both the low-cost instrument and the commercial instruments, one after the other, with each measurement being repeated thrice. The measurements were done during different time of the day in order to capture the current/voltage data at different irradiation and temperatures. Figure 4.3 shows the major setups for the outdoor current/voltage measurements.

Figure 4.3. Instruments and solar PV modules during outdoor measurements

.

In fig. 4.3, Label (1) shows the unremovable Solar World modules; label (2) are the irradiation sensors; label (3) is the PVPM1040C Commercial current/voltage tester; label (4) are the Cables and hardware for reading the measured data; label (5) is the Trina module under test and label (6) shows the Low-cost current/voltage tester and its power bank.

4.2 Equipment and software

4.2.1 The PVPM1040C I-V tester

The PVPM1040C solar current/voltage tester is one of three solar current/voltage testers used in this work. It is a commercial current/voltage tester manufactured by PV-Engineering GmbH. It has the capability of measuring current/voltage curves of both solar PV module and strings and can measure voltage up to 15000Vdc and a current up to 40Adc. Its measurement technique is based on the capacitive load method, which is highlighted in chapter 2. The capacitive load method is one of the widely used methods in commercial solar current/voltage testers. The PVPM1040C current/voltage tester has a small PC/tablet that can automatically save the measured data and also display the current-voltage or power-voltage curves. The measured data can be copied and transfer from the device using a USB drive or other devices.

Figure 4.4. PVPM1040C commercial I-V tester along with other hardware and cables

4.2.2 The low-cost I-V tester

Solar PV diagnostics and current-voltage curve measurement are usually done using commercial instruments. However, commercial instruments are very expensive and takes considerable space for its setup. Consequently, alternative measuring tools are being researched and developed with the goal of making current/voltage tester affordable and accessible for local researchers and engineers. It is against this backdrop that the low-cost current/voltage tester used in this work was developed at the institute of photovoltaics, university of Stuttgart. This low-cost tester uses the dc-dc convertor technique and a microcontroller for its current/voltage curve measurement. Similar to the PVPM1040C commercial current/voltage tester, it can measure the current/voltage curve of both a single solar module and an entire string. It is equipped with a power bank, temperature and irradiation sensors as well as connecting cables. Unlike the commercial instrument that has complex parts and need more time and experts for its operation, the low-cost instrument can be carried, setup, and operated with ease. Furthermore, the low-cost tester can automatically display and save its current/voltage data on any android phone or tablet using the pydriod 3 app. The pydriod 3 app is a downloadable app on Google playstore that can be used to execute python codes, display graphs, and perform numerals calculations. It operates without internet data when used with the low-cost instrument.

Figure 4.5 shows the low-cost current/voltage tester along with its sensors cables and power bank.

Figure 4.5. ipv low-cost solar PV Current-Voltage curve tracer

4.2.3 The WaveLabs SINUS-300 PRO Solar PV TESTER

The WaveLabs SINUS-300 PRO SOLAR PV tester is a sophisticated and large instrument for solar module characterization. Unlike the previously mentioned testers that measure solar PV systems outdoor, the WaveLabs solar PV tester operates indoor. It can be controlled from a computer using an accompanying software known as WAVELABS. Unlike other indoor solar PV testers that use Xenon lamps, the Wavelabs sinus-300 Pro is equipped with light emitting diodes (LED) that can seamlessly simulate the solar spectrum. It can measure a solar module in less than 500 microseconds by flashing its LEDs on the solar module, using a single click on the computer. After each measurement is completed, the information are stored and displayed on the Wavelabs software. The software can characterize the solar modules, displaying information such as the short circuit current, the open circuit voltage, the maximum power, the fill factor and the current-voltage graph. Despite its sophistication, one major disadvantage of this instrument compared to the low-cost tester is that its measure only a single solar module at a time, unlike the low-cost tester that can measure both a single module and a string.
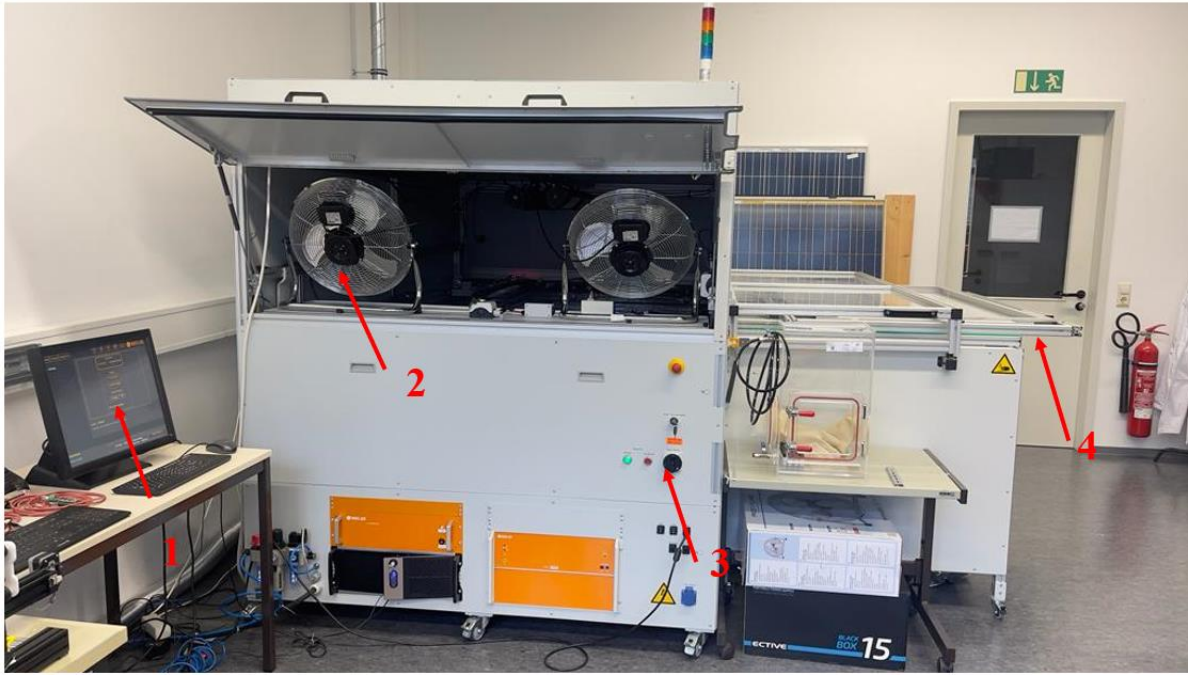
Figure 4.6. WAVELAB's SINUS-300 PRO Solar PV TESTER at ipv, University of Stuttgart

.

Figure 4.6 shows the external view of the sinus -300 Pro solar PV tester and some major components. In the figure, Label (1) represents the Wavelabs software displayed on the computer; label (2) shows the fans which are used to regulate the effect of external temperature during measurement; label (3) shows the main switch that is used for powering or turning off the instrument; and label (4) shows a solar module loaded from the right side of the instrument.

After loading the solar module unto the instrument as shown in label 4, it is automatically carried inside the instrument by a single mouse click on the loading function of the software in label 1.

4.2.4 Software for Data processing and evaluations

The measured current-voltage data were collected and transfer from each I-V tester to a computer using a USB hard drive.

The OriginLab software was the main software for the cleaning, processing and evaluations of the measured data while excel was used to collect and perform preliminary cleaning of the data. "Origin" is one of the best graphing and data analysis software in contemporary research. Because of its user-friendly interface, it can easily graph and perform analyses that would require complex procedures in other data analysis software such as "R" and python.

With "Origin", it was easy to clean data, smoothen graphs, remove noisy data points and extrapolated where necessary. The data from the low-cost instrument were cleaned and processed using moving average or adjacent average and the extrapolation functions in "Origin" software as their original current/voltage curves had a lot of noisy points and could not attain short circuit condition. In addition, data from the commercial instrument had less noisy points and all plots were evaluated, and their data extracted using the Werner evaluation method introduced in chapter 3.

Chapter 5. Experimental Results and Discussions

This section presents the findings and discussions of the experimental results obtained. First, a comparison of both the commercial and low-cost solar current/voltage testers is done with reference to their specifications and characterization. Next, the current/voltage curves of the measured solar modules as well as their respective Werner plots are presented and discussed. Furthermore, all values of the solar modules and cells parameters that were obtained from the plots are tabulated and discussed. The extraction methods for each parameter are discussed in chapter 3 and chapter 4 and are further elaborated in this section.

Table 5.1. Comparison of commercial and low-cost solar PV testers.

Company	product	I-V Measurement Technique	Range	Sweep speed	Total Data points	Single Module	String	Price(US$)
WAVELAB's	SINUS-300 PRO Solar PV TESTER	4-Quadrant method	60V, 20A	20-500μs	101	yes	no	50,000
ipv	Low-cost I-V tester	DC-DC Converter method	1000V, 20A	6s	901	yes	yes	1500
PV Engineering GmbH	The PVPM1040C I-V tester	Capacitive Load method	1000V, 40A	0.02-2s	101	yes	yes	4000

Table 5.1 draws a comparison amongst the three (3) instruments that were used for the measurement of the solar modules based on their specifications and characteristics. In the table, the measurement technique refers to the method that is used by each instrument to measure and display current/voltage data and graphs. These techniques have been reviewed in chapter 2. "Range" refers to the maximum and minimum values of current and voltage that each instrument is capable of measuring; The sweep time is the time taken for each instrument to complete a single measurement of the current/voltage curve between the short circuit current and the open circuit voltage; "string" indicates whether each instrument the instrument can measure more than one module connected in series or parallel while the data points refer to the total pair of current/voltage data that the instrument is capable of measuring. All these indicators are important when choosing which solar PV tester to buy or use.

In the table, the commercial solar PV tracers have advantage over the low-cost tracer mainly in terms of the measurement technique and sweep speed. The methods used by the commercial tracers are the most advanced and widely used method in the solar PV curve tracer market. Nevertheless, dc-dc converter method, which is the method used in the low-cost instrument, has also been used in commercial I-V tester such as EKO MP-180 (Zhu & Xiao, 2020). Furthermore, the sweep time of the low-cost instrument (6s) is in the acceptable range (2 to 300s) for I-V tracer on the market.

Aside from the sweep speed and the measurement techniques, the measurement range is another indicator associated with a good current/voltage tester. As seen in table 5, the low-cost instrument can measure voltage and current at higher ranges compared to the sophisticated Wavelabs instrument. This is so because the low-cost instrument is capable of measuring more than one solar modules while the Wavelabs instrument is only able to measure single modules at a time. Finally, the total number of data points that can be captured by the low-cost instrument shows another advantage. It can measure more than 8 times the number of data points measured by the commercial instruments. This indicator can give more information about the I-V curve. However, very large number of data points can sometimes be the reason for many noises and small ripples on the measured current/voltage curve.
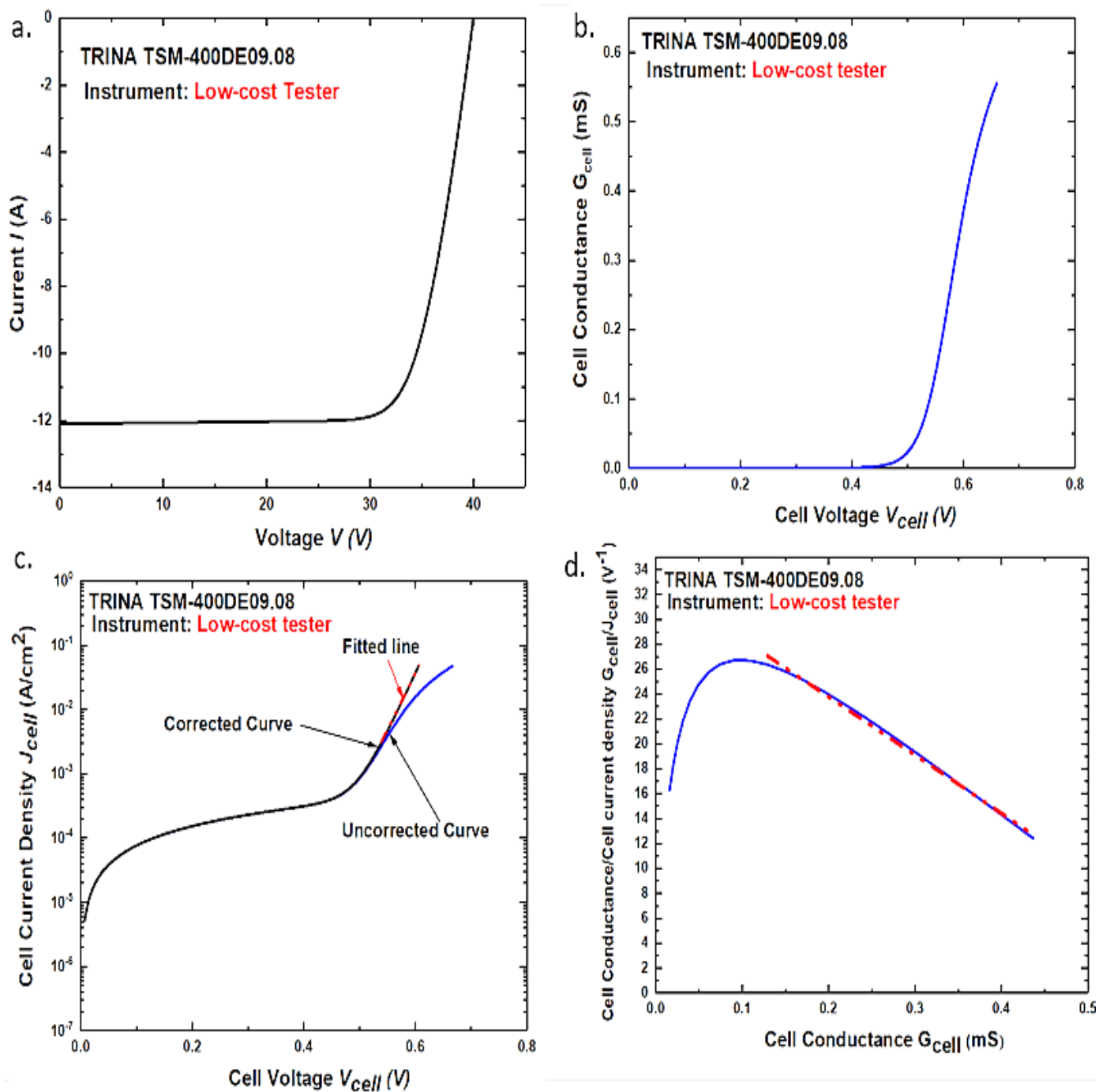
5.1 Results for the low-cost tester

Figure 5.1. Werner plots for the Trina solar modules obtained with the low-cost tester.

5.1.1 Interpretation of plots

Due to the similarities of in shapes of the Werner plots, Figures. 5.1, 5.2 and 5.3, are generally described to help better understand each plot in the figures. The plots in each figure appear similar in shape because they were plotted using similar methods. However, the main difference for each plot lies within the region and data points for which each calculated solar cell and module parameter was evaluated and the limit of the curves relative to their axes' values. For example, in fig. 5.1b, the conductance vs. voltage curve rises only for voltages greater than 0.5volts while a similar curve in fig.5.2b rises only for values beyond 0.7volts. Moreover, these differences are due to the characteristics of the modules, the technique and the limit of data points that the measuring instrument can read.

With this being noted, figures 5.1, 5.2 and 5.3(a to d) show the four (4) most important plots from which the solar module and cell parameters where extracted. Plot "a" of each figure shows the current/voltage plot from which the parallel resistances of the module were obtained; "b" shows how the cell conductance changes relative to its voltage. Nevertheless, this change is very small to be detected when the plot is done on a linear scale; hence, the curve is flat for voltages between 0-0.5Volts except for figure 5.2b where the maximum voltage value is 0.7. Beyond this range the curve begins to rise. Fig. 5.1, 5.2, and 5.3 (c) is the semilogarithmic plot showing the deviation of the "uncorrected curves" from the black curves due to the effect of their respective series resistance. This deviation is only noticeable at higher voltages as both the corrected and uncorrected curves appear as a single curve at low voltages. "Uncorrected curve", as used in the figures, indicates that the effect of series resistance has not yet been removed or subtracted from the respective curves; the higher the magnitude of this series resistance, the more pronounced is the deviation of the "uncorrected curves". This series resistance value was obtained from the curves in fig. d. and used to "correct" the "uncorrected curves. Once the effect of series resistance is removed, the region where the "uncorrected curves" bend becomes linear. This linear part of the curve is fitted to obtain the saturation current density J_o values and ideality factor n_1.

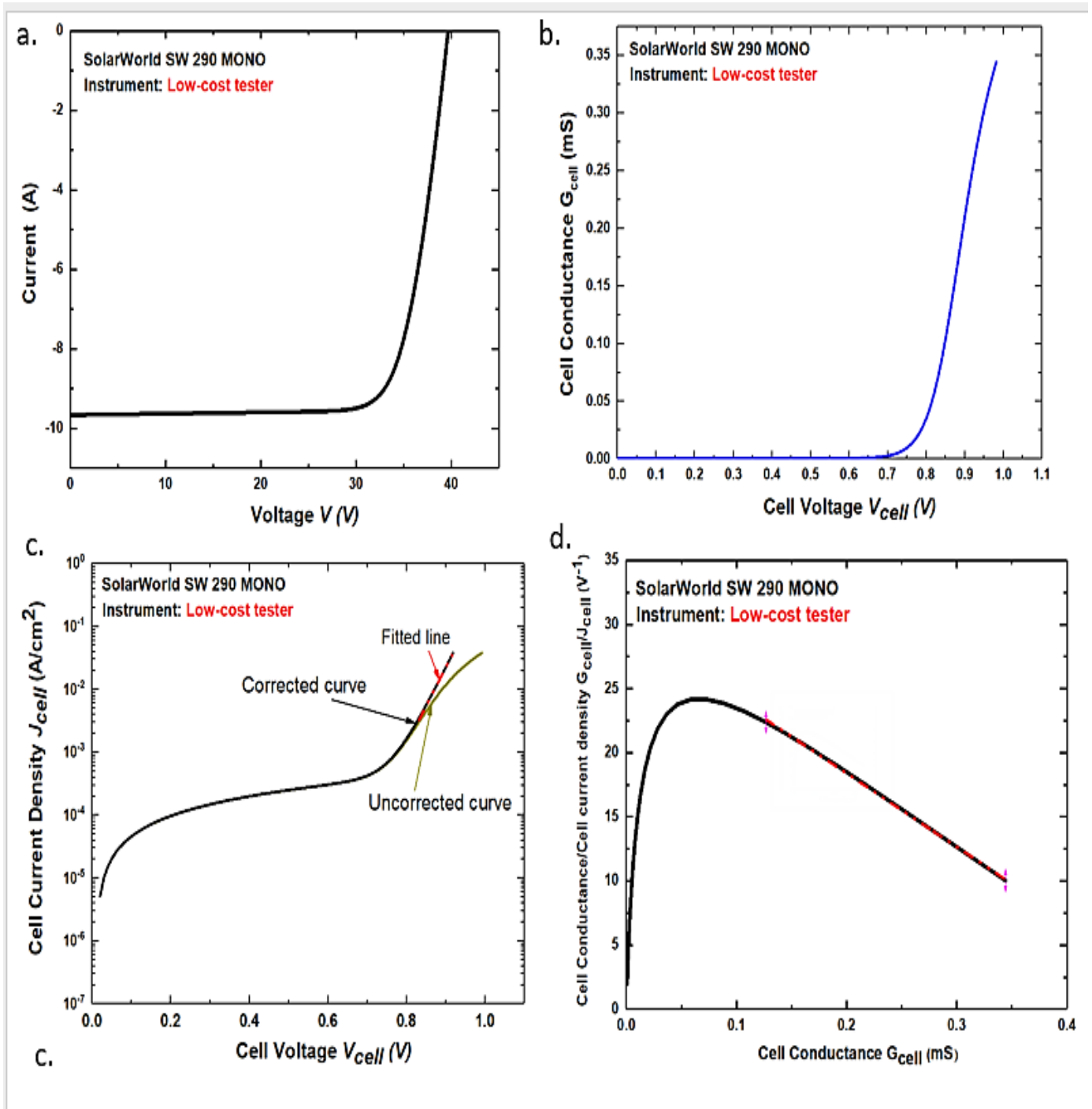All calculated parameters for fig. 5.1 to 5.3 are tabulated in table and discussed.

Figure 5.2 Werner plots for the SolarWorld modules obtained with the low-cost tester
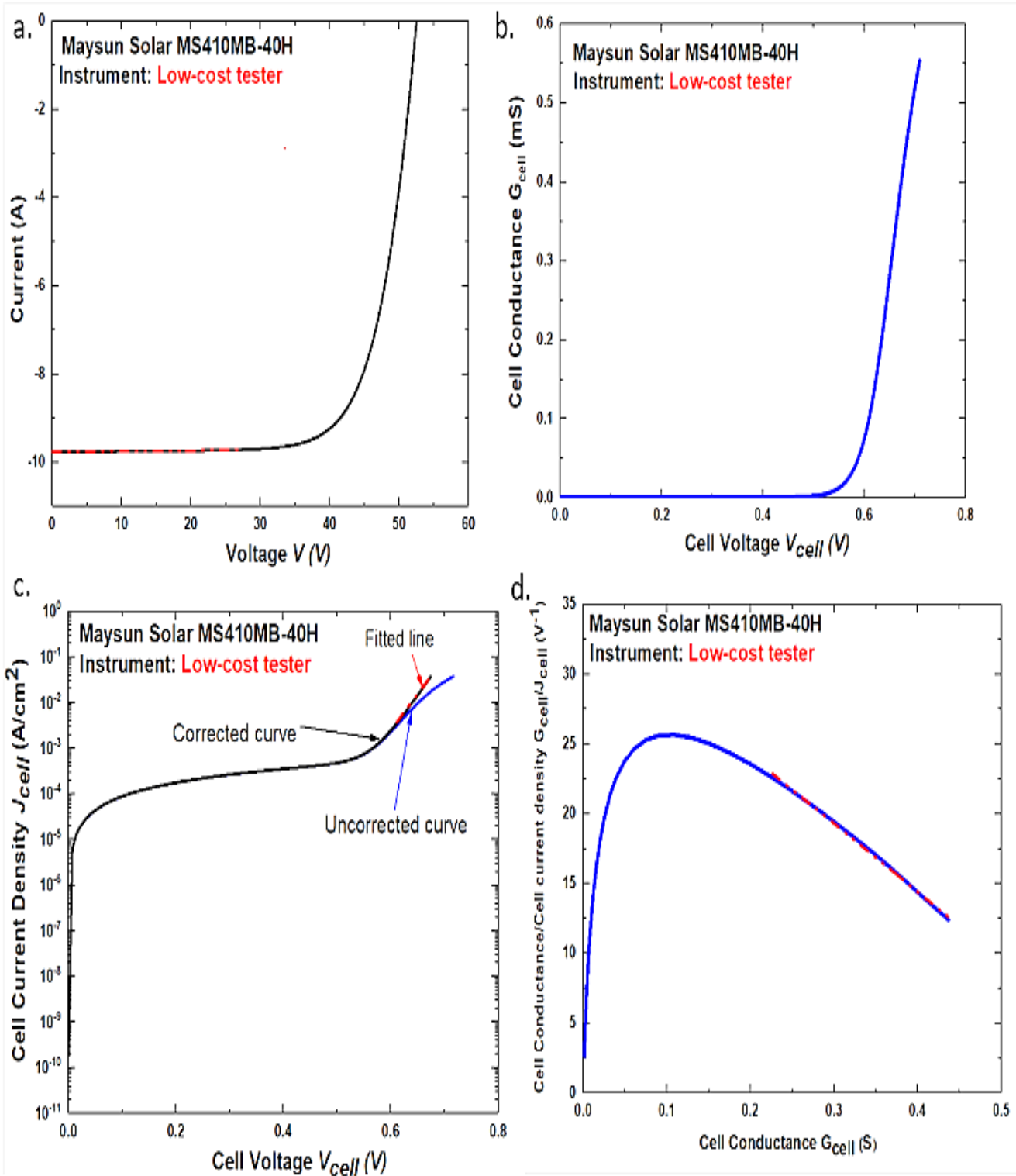
Figure 5.3. Werner plots for the Maysun solar modules obtained with the low-cost tester.

Table 5.2. Solar cell and module parameters for the low-cost instrument extracted from the modules in fig.5.1, fig 5.2, and fig.5.3

Name of module	Series resistance of cell $R_{s(cell)}$ [Ω cm^2]	Series resistance of module $R_{s(module)}$ [Ω]	Parallel resistance of cell $R_{p(cell)}$ [Ω cm^2] $\times 10^3$	Parallel resistance of module $R_{p(module)}$ [Ω] $\times 10$	Ideality factor n_1 First method	Ideality factor n_2 Second method	Saturation Current Density J_o [mA/cm^2]
Trina TSM-400DE09.08	1.42	0.29	1.29	30.6	1.21	1.15	2.87×10^{-10}
SolarWorld Plus Sw 290 Mono	1.92	0.47	1.95	30.5	1.34	1.32	6.67×10^{-13}
Maysun MS410MB-40H	1.44	0.52	1.12	63.7	1.18	1.04	2.67×10^{-15}

Table 5.2 present the results for the low-cost instrument. The series resistance of the cell $R_{s(cell)}$, measured in ohms centimeter square, is known as the area normalized series resistance and depends on the area of the cell. To obtain the absolute series resistance in ohms, eq. (16) was adopted.

Series Resistance of module $R_{s(module)}$

$$= \frac{Area\ normalized\ Series\ resistance\ of\ cell}{Area\ of\ cell} \times \frac{No.of\ cell\ in\ series}{No\ of\ cell\ in\ parallel} \quad (16)$$

For the results in table 5.2, the Trina module has the lowest series resistance per module and per cell, indicating a better electrical performance compared to the Maysun and Solarworld modules. Also, the Trina and the Maysun modules have relatively lower ideality factors in both methods one and two, indicating a better quality of the modules compared to the Solarworld module. Furthermore, the Trina module has the lowest saturation current density amongst the three solar modules. Lower value of the saturation current density of a solar cell or module implies a lower recombination rate and a low leakage current. Thus, from the result of the low-cost instrument, the Trina module has best performance in terms of series resistance, ideality factor and saturation current density while the Solarworld module is the worst performing module.

5.2 Results for the PVPM1040C commercial tester
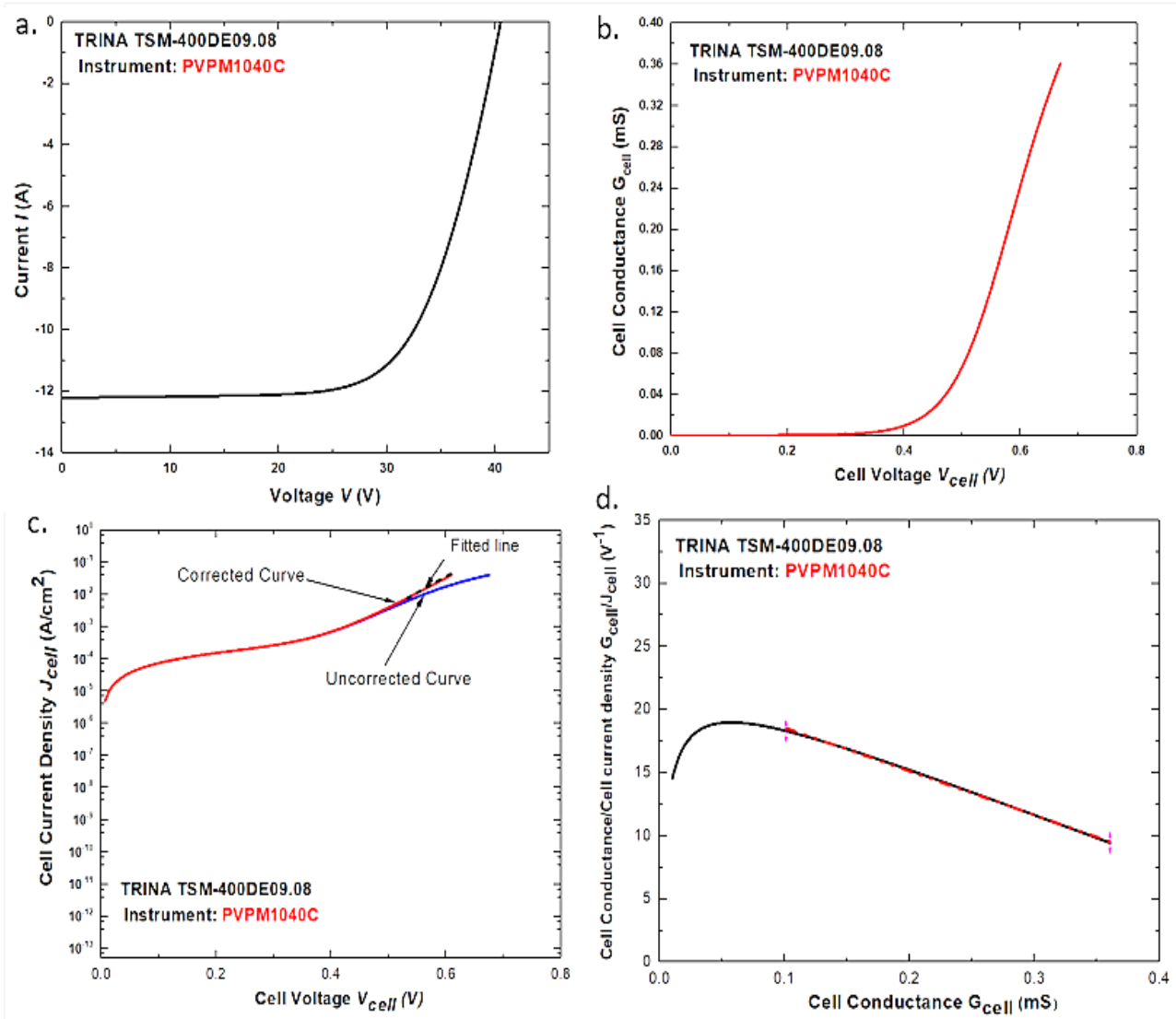
Figure 5.4. Werner plots for the trina solar modules obtained with the PVPM1040C commercial tester

Figures 5.4 to 5.6 show the plots for the three outdoor solar modules using the PVPM1040C commercial tester. An in-depth description of the function of each plot can be found under section 5.1.1 of this section and the results for all the extracted solar cells and modules parameters are given in table 5.3.
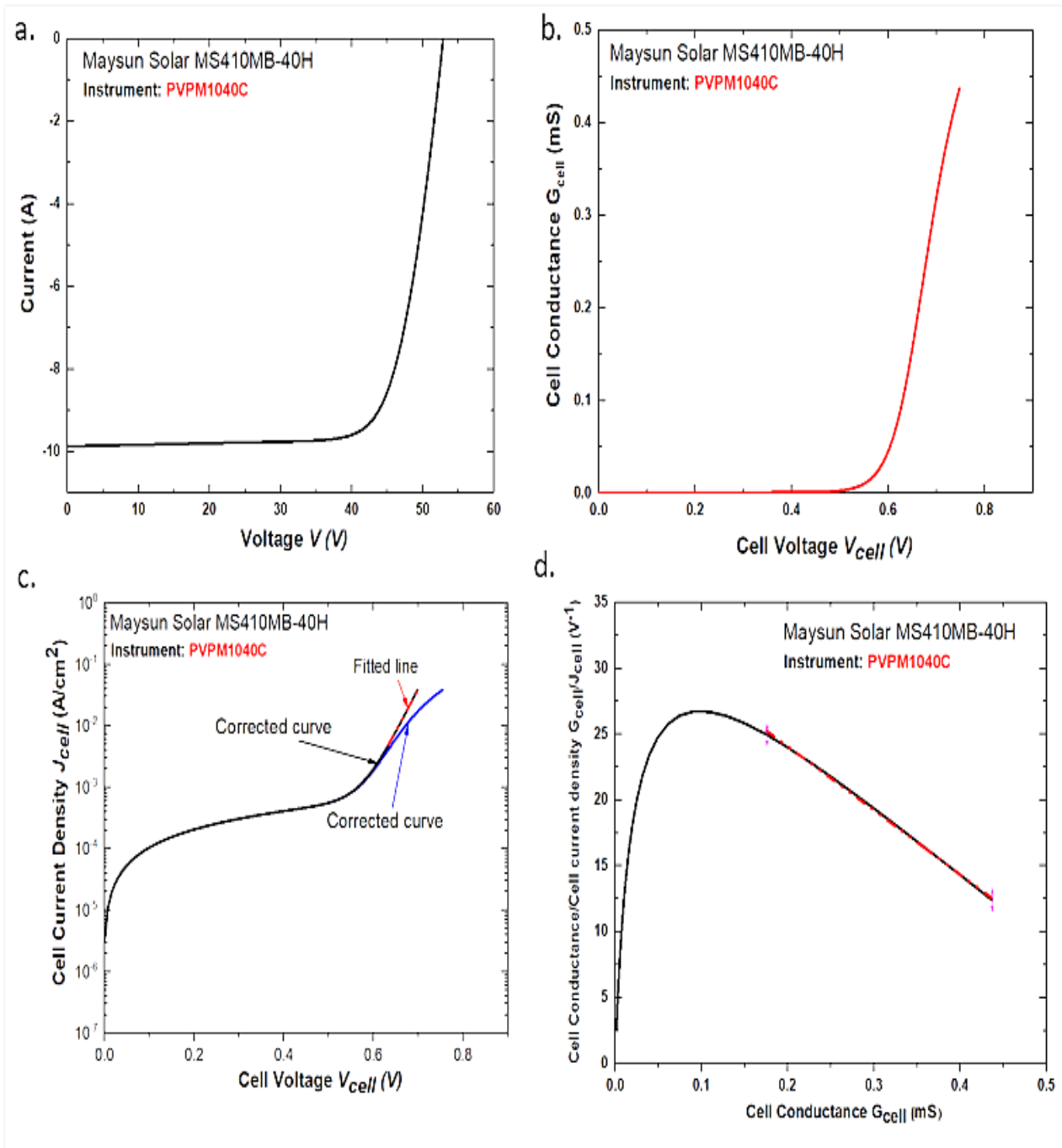
Figure 5.5. Werner plots for the maysun solar modules obtained with the PVPM1040C commercial tester
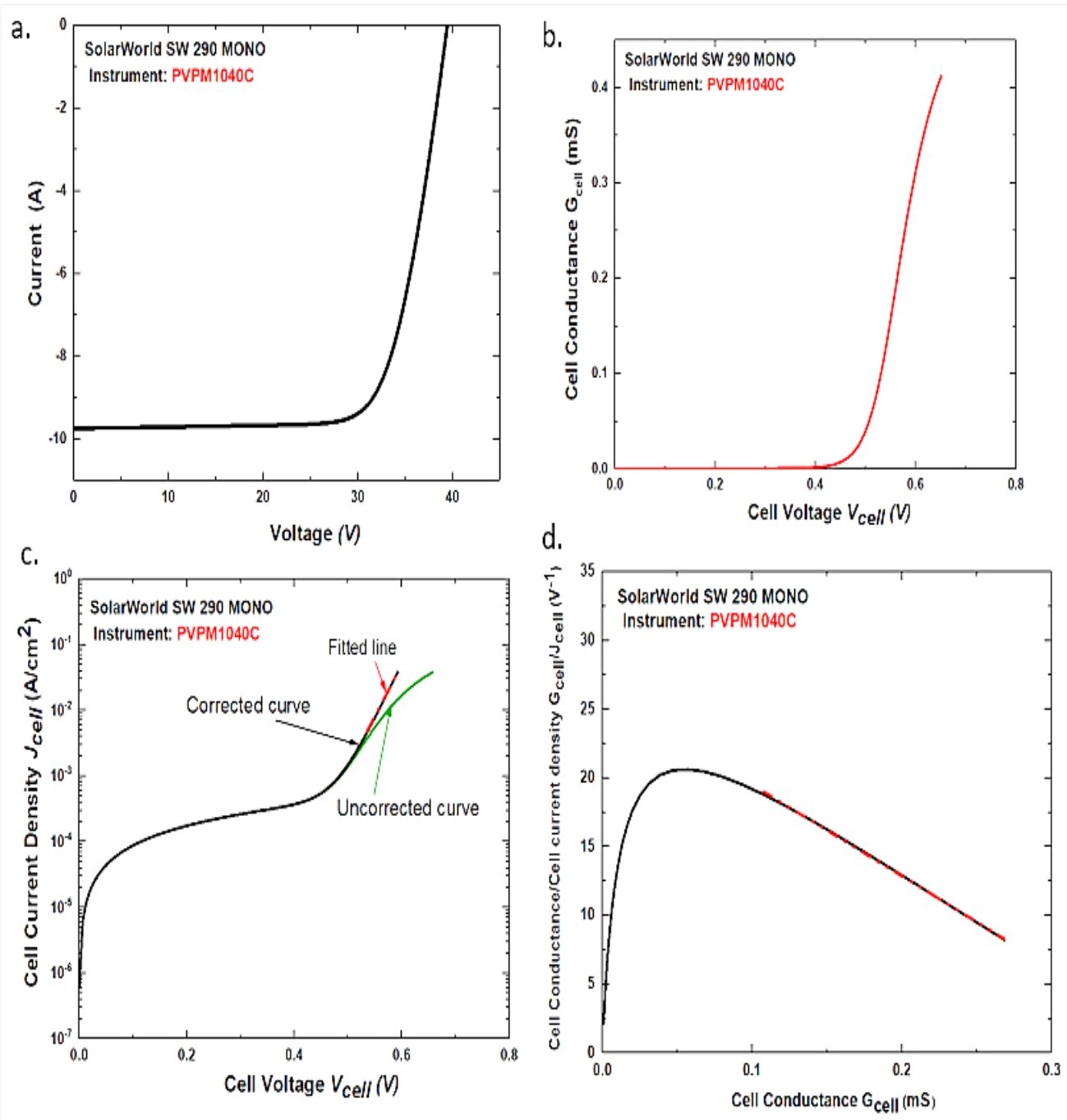
Figure 5.6. Werner plots for the solarWorld modules obtained with the PVPM1040C commercial tester

Table 5.3. Solar cell and module parameters for the PVPM1040C commercial tester extracted from the modules in fig.5.4, fig. 5.5, and fig.5.6.

Name of module	Series resistance of cell $R_{s(cell)}$ $[\Omega \text{ cm}^2]$	Series resistance of module $R_{s(module)}$ $[\Omega]$	Parallel resistance of cell $R_{p(cell)}$ $[\Omega \text{ cm}^2]$ $\times 10^2$	Parallel resistance of module $R_{p(module)}$ $[\Omega]$ $\times 10$	Ideality factor n_1 First method	Ideality factor n_2 Second method	Saturation Current Density J_o $[\text{mA}/cm^2]$
Trina TSM-400DE09.08	1.438	1.041	*9.52*	2.70	1.18	1.22	1.21×10^{-11}
SolarWorld Plus Sw 290 Mono	1.573	0.321	8.00	2.19	1.81	1.35	2.11×10^{-7}
Maysun MS410MB-40H	2.542	0.629	3.42	2.68	1.51	1.06	2.10×10^{-11}

Table 5.3 presents the results for the solar cells and modules parameters for the PVPM1040C commercial I-V tester for Fig.5.4, Fig.5.5, and Fig.5.6. From the results, the trina module has the smallest series resistance when compared to the Maysun and solarWorld modules. This result for trina with the commercial instrument is consistent with the result obtained for trina using the low-cost instrument. However, the measured series resistance for the Maysun module is larger in the case of the commercial instrument as opposed to the low-cost instrument. Furthermore, the shunt resistances obtained for the three modules are significantly lower when compared to those obtained with the low-cost ipv measurement unit. Nevertheless, the trina and maysun modules have better performances in terms of saturation current density, when measured with the PVPM1040C commercial I-V tester as well as the low-cost tester.

5.3 Results for the WaveLabs SINUS-300 PRO commercial PV tester
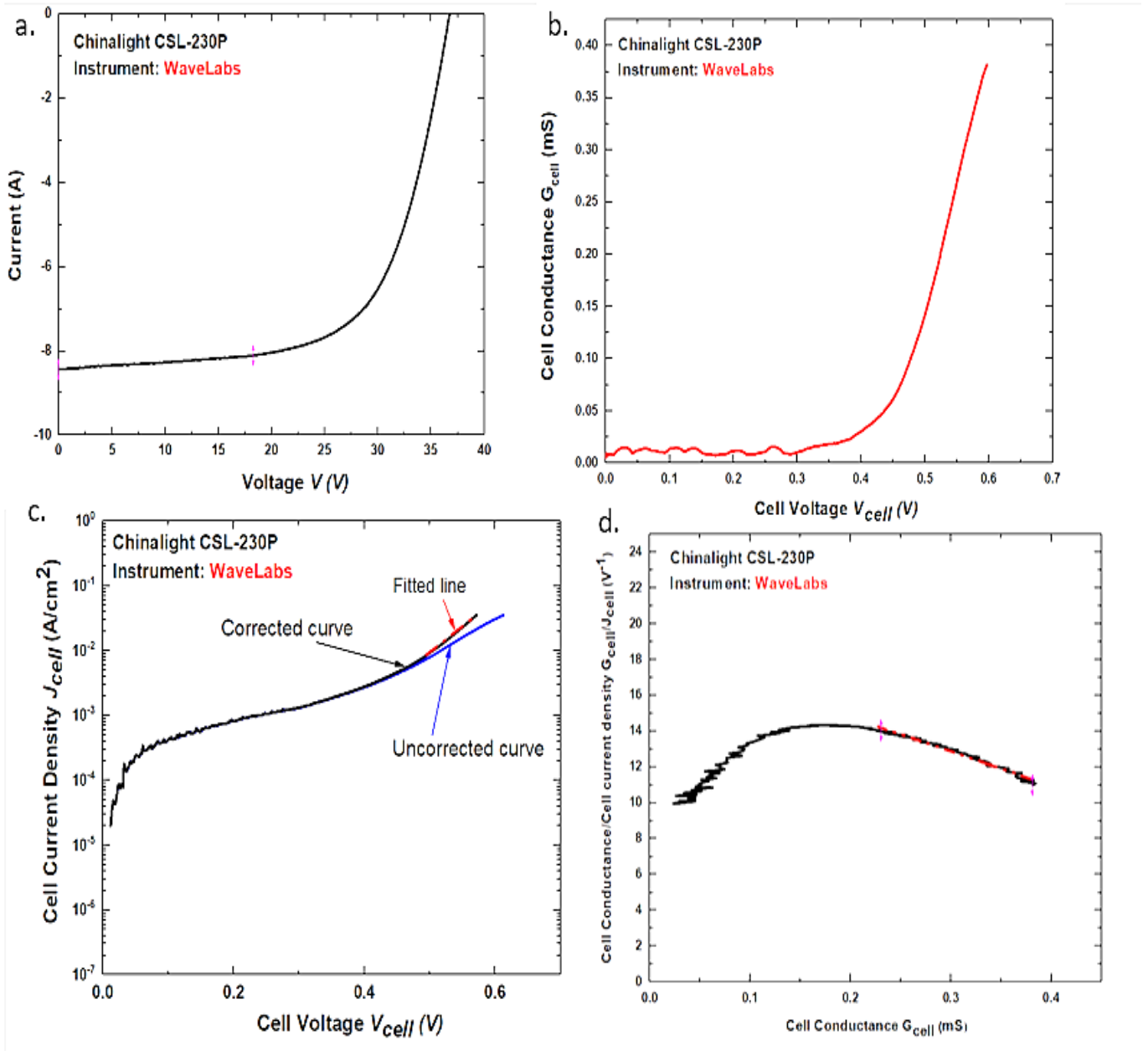
Figure 5.7. Werner plots for the Chinalight modules obtained with the WaveLabs commercial tester

Figures 5.7 and 5.8 show the results for the plots for the China light solar module measured indoor with Wavelabs. The ripples on the curves in Fig. 5.7 give a quick insight about the performance of the modules. It reveals bad data points on the curve that are caused by the high degradation of modules the Chinalight module.
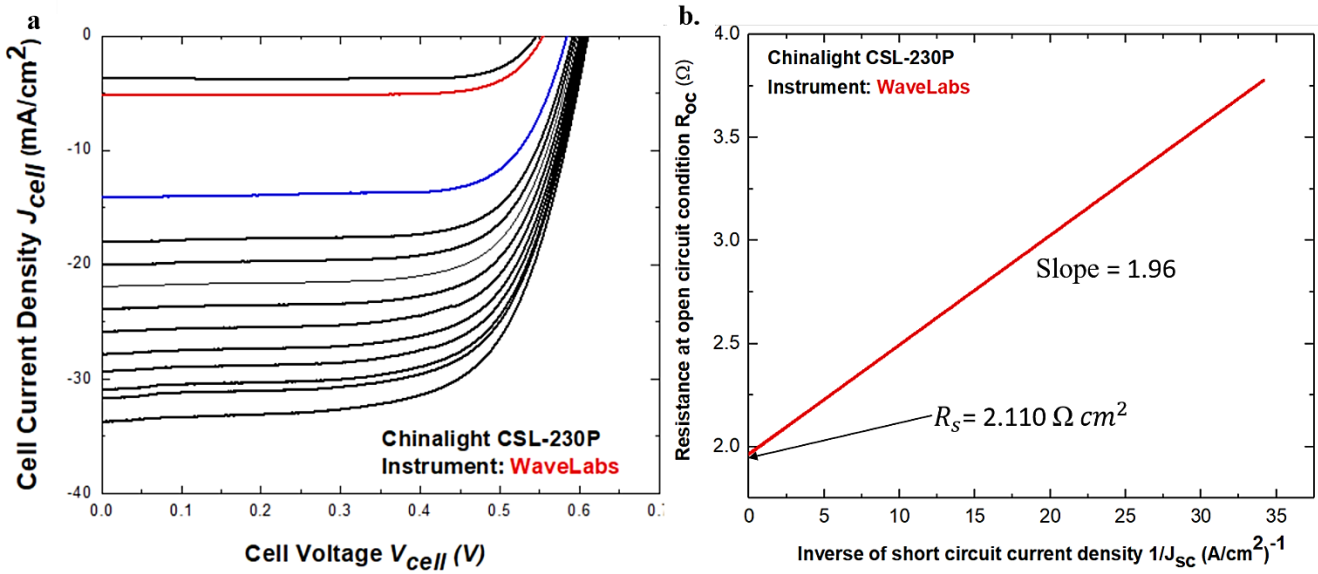
Figure 5.8. a. J-V curves of the China light modules at different illuminations   b. Third method of determining ideality factor and series resistance.

Figure 5.8a. shows several current/voltage curves for the Chinalight module measured at different illuminations.   This was achieved by varying the illumination values from highest to smallest.   The   aim was to demonstrate the third method for calculating series resistance and ideality factor according to the Werner method. This was done by extracting the short circuit current density of the curves and the slopes near open circuit conditions. The inverse of slope of the current/voltage curve of a solar module at open circuit condition is often reported as the series resistance of the module. The eq. (9) of the Werner method (chapter 3) demonstrates that this method of determining series resistance is completely wrong; hence, the correct method to determine the series resistance, using the resistance at open circuit voltage is by taking the inverse of the slope R_{oc} for each curve in fig.33a at open circuit voltage and plot them against the inverse of the short circuit current density J_{sc}^{-1} . The result should a straight line whose slope give the ideality factor and whose y-intercept gives the series resistance as seen in Fig. 5.8b.
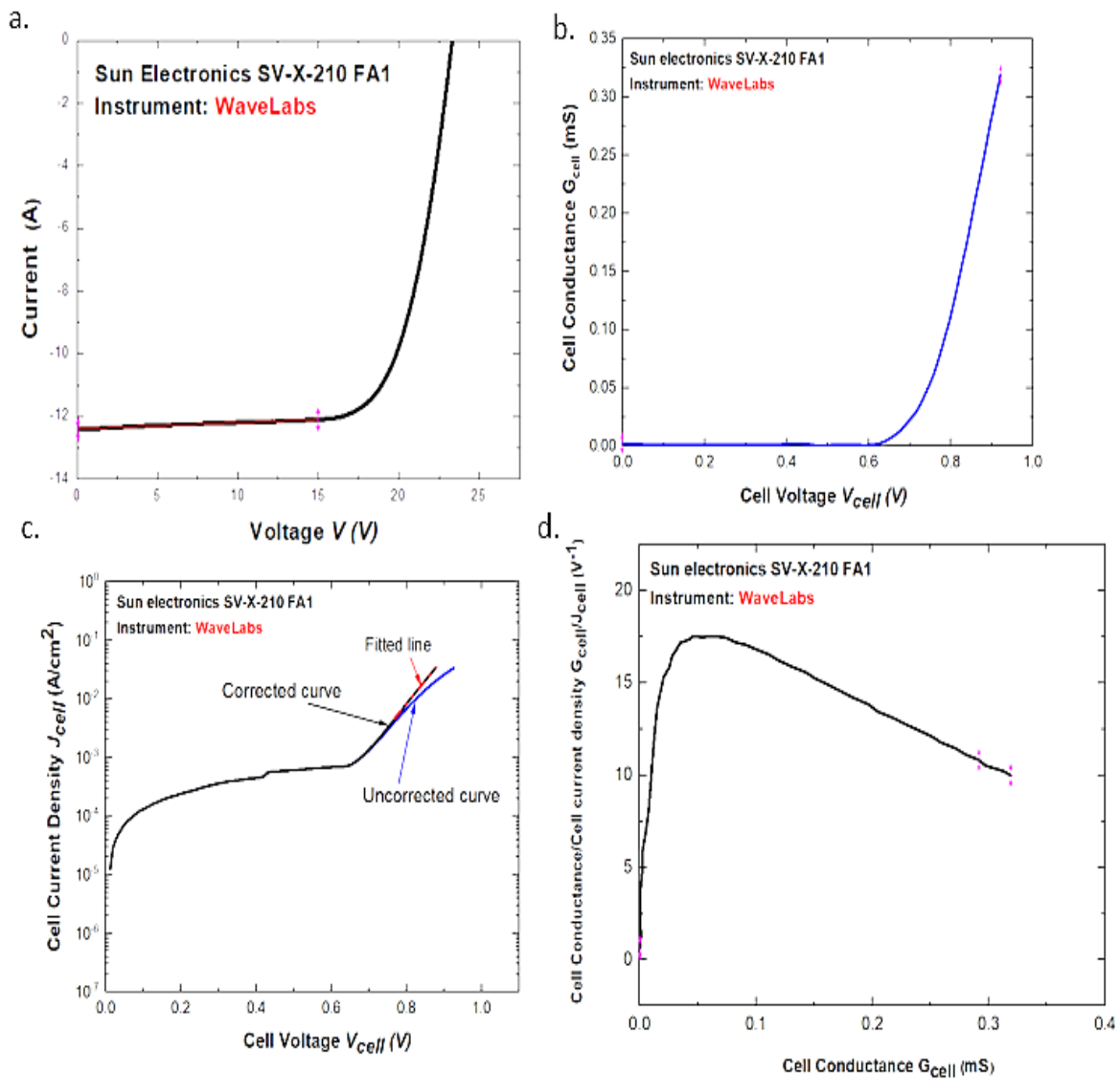
Figure 5.9. Werner plots for the Sunelectronic modules obtained with the WaveLabs commercial tester
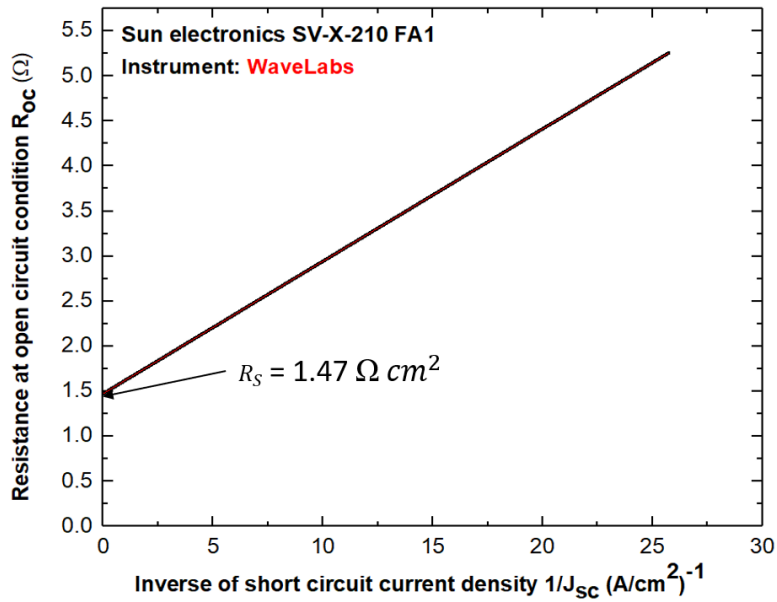
Figure 5.10. Third method for series resistance and ideality factor for the sun electrons module

Table 5.4. Wavelabs results for chinalight and Sunelectronics modules

Name of module	Series resistance of cell $R_{s(cell)}$ $[\Omega\,cm^2]$	Series resistance of module $R_{s(module)}$ $[\Omega]$	Parallel resistance of cell $R_{p(cell)}$ $[\Omega\,cm^2]$ $\times 10$	Parallel resistance of module $R_{p(module)}$ $[\Omega]$	Ideality factor n_1 First method	Ideality factor n_2 Second method	Ideality factor n_3 Third method	Saturation Current Density J_o $[mA/cm^2]$
Chinalight CLS-230P	2.06	1.03	21.0	57.8	2.11	2.05	1.96	1.29×10^{-6}
Sun electronics SV-X-210 FA1	1.47	0.311	10.6	50.1	2.12	2.17	2.160	8.88×10^{-9}

Table 5.4 shows that sun electronics has lower series resistance for both modules and cells, indicating a better electrical performance compared to chinalight. Both chinalight and sunelectronics have higher ideality factor for all three methods. These values for ideality factor are the highest for all the measured modules. Moreover, the shunt resistances for both modules are the lowest in all cases. Hence, chinalight and sunelectronics have the least performance for the three instruments and all the measured module.

Table 5.5. Modules back cables parameters and resistance.

Parameters of modules's back cables	Trina TSM-400DE09.08	Maysun MS410MB-40H	SolarWorld Plus Sw 290 Mono	Chinalight CLS-230P	Sun electronics SV-X-210-FA1
Length of cables **[cm]**	110	70	118	96	108
Cross-sectional areas of cables (**mm^2**)	6	6	6	6	6
Resistance (**Ω)**	$3.2.\times 10^{-4}$	2.0×10^{-2}	3.4×10^{-4}	2.75×10^{-3}	3.1×10^{-4}

Table 5.5 shows the characteristics and resistance of the back cables of each measured solar module. The back cables of a solar module collect current produced by the module and transfer it the external circuit. Normally, the back cables offer some level of resistance which can increase the total series resistance of the module except they are optimized to minimized resistance during their production. The resistance of the cables depends on the length of the cable *l*, the quality of the cable, and the diameter. Each resistance value was obtained using the equation,

$$R_C = \rho l/A, \tag{17}$$

where R_C is the resistance of the cable, A denotes the cross-sectional area of the cable and

$\rho = 1.72 \times 10^{-8} \ \Omega - m$ is the resistivity of the cable.

Results from table 5.5 show that the contribution of the back cables to the series resistance is far less than the internal series resistance of the modules. Thus, it can be concluded that the back cables do not contribute significantly to the series resistance of the modules.

6. Conclusion

Solar PV module parameters are significant indicators for the performance of solar PV modules. Their evaluations can help scientists, engineers, researchers and solar installers to make important decisions about the design and optimization of solar modules or cells. To evaluate solar module or cell parameters, the current/voltage curve data must be measured. However, the current/voltage curve measurement is usually done using commercial current/voltage curve testers that are very expensive to be accessed by local institutions, solar installers and researchers. Consequently, researchers are beginning to develop alternative low-cost instruments to compete with commercial current/voltage curve tracers. Hence, to ascertain the merits and demerits of both commercial and low-cost current/voltage testers in measuring current/voltage curve of solar module, this thesis compared two sophisticated and expensive commercial current/voltage testers and a low-cost current tester developed at the institute for Photovoltaics(ipv), University of Stuttgart, by each group of each can be used to measure and extract solar module parameters. To achieve this, five solar modules were measured.

Generally, the experimental results show that the low-cost current/voltage tester results are competitive relative to the commercial instrument. For example, the result for the series resistance and saturation current density for the Trina module was consistent with the results obtained with the PVPM1040C commercial tester. Furthermore, PVPM1040C commercial tester showed a larger series resistance for the Maysun module as opposed to a smaller value with the low-cost tester. Nevertheless, raw(uncleaned) current/voltage data for the low-cost instrument showed more noise when compared to its sophisticated counterparts.

Therefore, the research results ascertained the competitiveness and viability of using alternative low-cost current/voltage tester for solar module current/voltage curve measurements. However, it should be mentioned that the low-cost instrument has certain limitations when compared to the commercial instrument. Unlike the commercial instruments that use digital filters to minimize noisy data points during measurement, the low-cost instrument lacks a digital filter. This makes the raw current/voltage data of the low-cost instrument extremely noisy, demanding thorough data cleaning before use.

6.1 Perspective for future work

This research has shed light on the abilities of both low-cost and commercial current/voltage testers in measuring the current/voltage curves and solar module/cell parameters of photovoltaic modules. While the findings showed promising results for the low-cost instrument when compared to its sophisticated counterparts, it is important to address some key issues for future research with low-cost current/voltage testers. Hence, the following recommendations are presented:

1. **Noise Reduction:** As pointed out in this work, the current/voltage data obtained using the low-cost instrument had several noisy points. Future research could focus on noise reduction techniques or the development of digital filters to help reduce noise in low-cost instruments.

2. **Improvement of Accuracy:** future work should continue to improve the accuracy of low-cost current/voltage testers. This could be achieved by creating advanced sensor technologies and hardware components as well as following standard calibration protocols.

3. **Standardization:** low-cost testers should be developed to meet industrial standards and classifications. This will increase reliability as industries and big companies could begin to use low-cost current/voltage testers

4. **The Application of Low-Cost Testers in Emerging Solar Technologies:** it important apply low-cost current/voltage testers in measuring emerging solar technologies such as perovskite and bifacial solar modules to ascertain their accuracy and reliability.

6.2 References

1. Aberle, A. G., Zhang, W., & Hoex, B. (2011). Advanced loss analysis method for silicon wafer solar cells. *Energy Procedia*, *8*, 244–249. https://doi.org/10.1016/j.egypro.2011.06.131

2. Agarwal, S. K., Muralidharan, R., Agarwala, A., Tewary, V. K., & Jain, S. C. (1981). A new method for the measurement of series resistance of solar cells. *Journal of Physics D: Applied Physics*, *14*(9), 1643–1646. https://doi.org/10.1088/0022-3727/14/9/011

3. AlHajri, M. F., El-Naggar, K. M., AlRashidi, M. R., & Al-Othman, A. K. (2012). Optimal extraction of solar cell parameters using pattern search. *Renewable Energy*, *44*, 238–245. https://doi.org/10.1016/j.renene.2012.01.082

4. Ali, M. H., Rabhi, A., Hajjaji, A. E., & Tina, G. M. (2017). Real Time Fault Detection in Photovoltaic Systems. *Energy Procedia*, *111*, 914–923. https://doi.org/10.1016/j.egypro.2017.03.254

5. Bai, J., Liu, S., Hao, Y., Zhang, Z., Jiang, M., & Zhang, Y. (2014). Development of a new compound method to extract the five parameters of PV modules. *Energy Conversion and Management*, *79*, 294–303. https://doi.org/10.1016/j.enconman.2013.12.041

6. BELLINI, E. (2020, April 6). *World now has 583.5 GW of operational PV*. https://www.pv-magazine.com/2020/04/06/world-now-has-583-5-gw-of-operational-pv/

7. Bouzidi, K., Chegaar, M., & Aillerie, M. (2012). Solar Cells Parameters Evaluation from Dark I-V Characteristics. *Energy Procedia*, *18*, 1601–1610. https://doi.org/10.1016/j.egypro.2012.06.001

8. Cáceres, M., Firman, A., Montes-Romero, J., González Mayans, A. R., Vera, L. H., F. Fernández, E., & de la Casa Higueras, J. (2020). Low-Cost I–V Tracer for PV Modules

under Real Operating Conditions. *Energies*, *13*(17), 4320. https://doi.org/10.3390/en13174320

9. Chegaar, M., Azzouzi, G., & Mialhe, P. (2006). Simple parameter extraction method for illuminated solar cells. *Solid-State Electronics*, *50*(7–8), 1234–1237. https://doi.org/10.1016/j.sse.2006.05.020

10. Chegaar, M., Ouennoughi, Z., & Guechi, F. (2004). Extracting dc parameters of solar cells under illumination. *Vacuum*, *75*(4), 367–372. https://doi.org/10.1016/j.vacuum.2004.05.001

11. Cholish, Sara, I. D., Away, Y., Azis, A., & Noorly, E. (2019). The current and voltage curves simulation solar module using IV tracer networks. *IOP Conference Series: Materials Science and Engineering*, *674*(1), 012033. https://doi.org/10.1088/1757-899X/674/1/012033

12. Cubas, J., & Pindado, S. (2014). *Explicit Expressions for Solar Panel Equivalent Circuit Parameters Based on Analytical Formulation and the Lambert W-Function †*.

13. Das, S. (2016). Development of a Low-cost, Portable, and Programmable Solar Module to Facilitate Hands-on Experiments and Improve Student Learning. *2016 ASEE Annual Conference & Exposition Proceedings*, 26800. https://doi.org/10.18260/p.26800

14. Durán, E., Andújar, J. M., Enrique, J. M., & Pérez-Oria, J. M. (2012). Determination of PV Generator *I-V/P-V* Characteristic Curves Using a DC-DC Converter Controlled by a Virtual Instrument. *International Journal of Photoenergy*, *2012*, 1–13. https://doi.org/10.1155/2012/843185

15. Durán, E., Andújar, J. M., Segura, F., & Barragán, A. J. (2011). A high-flexibility DC load for fuel cell and solar arrays power sources based on DC–DC converters. *Applied Energy*, *88*(5), 1690–1702. https://doi.org/10.1016/j.apenergy.2010.11.002

16. Duran, E., Piliougine, M., Sidrach-de-Cardona, M., Galan, J., & Andujar, J. M. (2008). Different methods to obtain the I–V curve of PV modules: A review. *2008 33rd IEEE Photovolatic Specialists Conference*, 1–6. https://doi.org/10.1109/PVSC.2008.4922578

17. Enrique, J. M., Duran, E., Sidrach-de-Cardona M, Andujar, J. M., Bohorquez, M. A., & Carretero, J. (2005). A new approach to obtain I-V and P-V curves of photovoltaic modules by using DC-DC converters. *Conference Record of the Thirty-First IEEE Photovoltaic Specialists Conference, 2005.*, 1769–1772. https://doi.org/10.1109/PVSC.2005.1488493

18. Firth, S. K., Lomas, K. J., & Rees, S. J. (2010). A simple model of PV system performance and its use in fault detection. *Solar Energy*, *84*(4), 624–635. https://doi.org/10.1016/j.solener.2009.08.004

19. Hiscocks, P. D., & Gaston, J. (2007). *Low-Cost Curve Tracer Uses PC-Based Scope. June 22, 2007*.https://www.bing.com/ck/a?!&&p=fb0b4ca7d4eb5760JmltdHM9MTY5MDMyOTY OTY

20. Isaac Morko Kwembur. (2013). *DESIGNING AND FABRICATION OF A CURRENT-VOLTAGE CURVE METER FOR ELECTRICAL CHARACTERIZATION OF PHOTOVOLTAIC MODULES.*

21. Isdawimah, Ismujianto, Oktariza, L. G., Frederik, A., & Phuoc Loc, N. (2019). Investigation of Photovoltaic System Parameters Using LabView in Solar Irradiance Peak Condition. *Journal of Physics: Conference Series*, *1364*(1), 012065. https://doi.org/10.1088/1742-6596/1364/1/012065

22. Ishaque, K., Salam, Z., & Taheri, H. (2011). Simple, fast and accurate two-diode model for photovoltaic modules. *Solar Energy Materials and Solar Cells*, *95*(2), 586–594. https://doi.org/10.1016/j.solmat.2010.09.023

23. Khan, F., Baek, S.-H., Park, Y., & Kim, J. H. (2013). Extraction of diode parameters of silicon solar cells under high illumination conditions. *Energy Conversion and Management*, *76*, 421–429. https://doi.org/10.1016/j.enconman.2013.07.054

24. Khatib, T., Elmenreich, W., & Mohamed, A. (2017). Simplified I-V Characteristic Tester for Photovoltaic Modules Using a DC-DC Boost Converter. *Sustainability*, *9*(4), 657. https://doi.org/10.3390/su9040657

25. Khunchan, S., & Wiengmoon, B. (2018). Method to determine the single curve IV characteristic parameter of solar cell. *Journal of Physics: Conference Series*, *1144*, 012012. https://doi.org/10.1088/1742-6596/1144/1/012012

26. Kongphet, V., Migan-Dubois, A., Delpha, C., Lechenadec, J.-Y., & Diallo, D. (2022). Low-Cost I–V Tracer for PV Fault Diagnosis Using Single-Diode Model Parameters and I–V Curve Characteristics. *Energies*, *15*(15), 5350. https://doi.org/10.3390/en15155350

27. Leite, V., Batista, J., Williams, R., Chenlo, F., & Afonso, J. L. (n.d.). *Determination of Model Parameters of PV Modules Using a Low Cost I-V Tracer*.

28. Londoño, C. D., Cano, J. B., & Velilla, E. (2022). Capacitive tracer design to mitigate incomplete I-V curves in outdoor tests. *Solar Energy*, *243*, 361–369. https://doi.org/10.1016/j.solener.2022.08.021

29. Mahmoud, M. M. (2006). Transient analysis of a PV power generator charging a capacitor for measurement of the I–V characteristics. *Renewable Energy*, *31*(13), 2198–2206. https://doi.org/10.1016/j.renene.2005.09.019

30. Mellit, A., Tina, G. M., & Kalogirou, S. A. (2018). Fault detection and diagnosis methods for photovoltaic systems: A review. *Renewable and Sustainable Energy Reviews*, *91*, 1–17. https://doi.org/10.1016/j.rser.2018.03.062

31. Mertens, K. (2014). *Photovoltaics: Fundamentals, technology and practice*. Wiley.

32. Morales-Aragonés, J. I., Dávila-Sacoto, M., González, L. G., Alonso-Gómez, V., Gallardo-Saavedra, S., & Hernández-Callejo, L. (2021). A Review of I–V Tracers for Photovoltaic Modules: Topologies and Challenges. *Electronics*, *10*(11), 1283. https://doi.org/10.3390/electronics10111283

33. Ouennoughi, Z., & Chegaar, M. (1999). A simpler method for extracting solar cell parameters using the conductance method. *Solid-State Electronics*, *43*(11), 1985–1988. https://doi.org/10.1016/S0038-1101(99)00174-4

34. Pereira, T. A., Schmitz, L., dos Santos, W. M., Martins, D. C., & Coelho, R. F. (2021). Design of a Portable Photovoltaic *I–V* Curve Tracer Based on the DC–DC Converter Method. *IEEE Journal of Photovoltaics*, *11*(2), 552–560. https://doi.org/10.1109/JPHOTOV.2021.3049903

35. Sayyad, J., & Nasikkar, P. (2021). Design and Development of Low Cost, Portable, On-Field I-V Curve Tracer Based on Capacitor Loading for High Power Rated Solar Photovoltaic Modules. *IEEE Access*, *9*, 70715–70731. https://doi.org/10.1109/ACCESS.2021.3078532

36. Smets, A. H. M., Jäger, K., Isabella, O., Swaaij, R. van, & Zeman, M. (2016). *Solar energy: The physics and engineering of photovoltaic conversion, technologies and systems*. UIT Cambridge.

37. Teyabeen, A. A., Elhatmi, N. B., Essnid, A. A., & Jwaid, A. E. (2020). Parameters Estimation of Solar PV Modules Based on Single-Diode Model. *2020 11th*

International Renewable Energy Congress (IREC), 1–6. https://doi.org/10.1109/IREC48820.2020.9310365

38. Van Dyk, E. E., Gxasheka, A. R., & Meyer, E. L. (2005). Monitoring current–voltage characteristics and energy output of silicon photovoltaic modules. *Renewable Energy*, *30*(3), 399–411. https://doi.org/10.1016/j.renene.2004.04.016

39. Werner, J. H. (1988). Schottky barrier and pn-junctionI/V plots？ Small signal evaluation. *Applied Physics A Solids and Surfaces*, *47*(3), 291–300. https://doi.org/10.1007/BF00615935

40. Willoughby, A. A., & Osinowo, M. O. (2018). Development of an electronic load I-V curve tracer to investigate the impact of Harmattan aerosol loading on PV module pern2tkformance in southwest Nigeria. *Solar Energy*, *166*, 171–180. https://doi.org/10.1016/j.solener.2018.03.047

41. World Energy Outlook 2020. Technical Report of International Energy Agency. 2020. Available online:https://iea.blob.core.windows.net/assets/a72d8abf-de08-4385-8711-b8a062d6124a/WEO2020.pdf (accessed on 26 July 2023)

42. Yaqoob, S. J., & Obed, A. A. (2019). *Modeling, simulation and implementation of photovoltaic panel model by proteus software based on high accuracy two- diode model*. *1*(1).

43. Yauri, R., & Espino, R. (2023). Embedded electronic system for evaluation of photovoltaic modules based on a current-voltage curve tracer. *Indonesian Journal of Electrical Engineering and Computer Science*, *29*(3), 1281. https://doi.org/10.11591/ijeecs.v29.i3.pp1281-1289

44. Zhu, Y., & Xiao, W. (2020). A comprehensive review of topologies for photovoltaic I–V curve tracer. *Solar Energy*, *196*, 346–357. https://doi.org/10.1016/j.solener.2019.12.020